進捗報告

2025/10/24

椊 昌孝

① 非可換ゲージ場（スピン軌道相互作用）のもとでの無秩序系の波動輸送

arXiv:2509.07312

② 平坦バンドとディラック点を有する$\alpha - T_3$格子におけるカイラルd波超伝導

Coherent backscattering (CBS)

Enhanced scattering probability in the opposite direction of incident wave (backscattering)

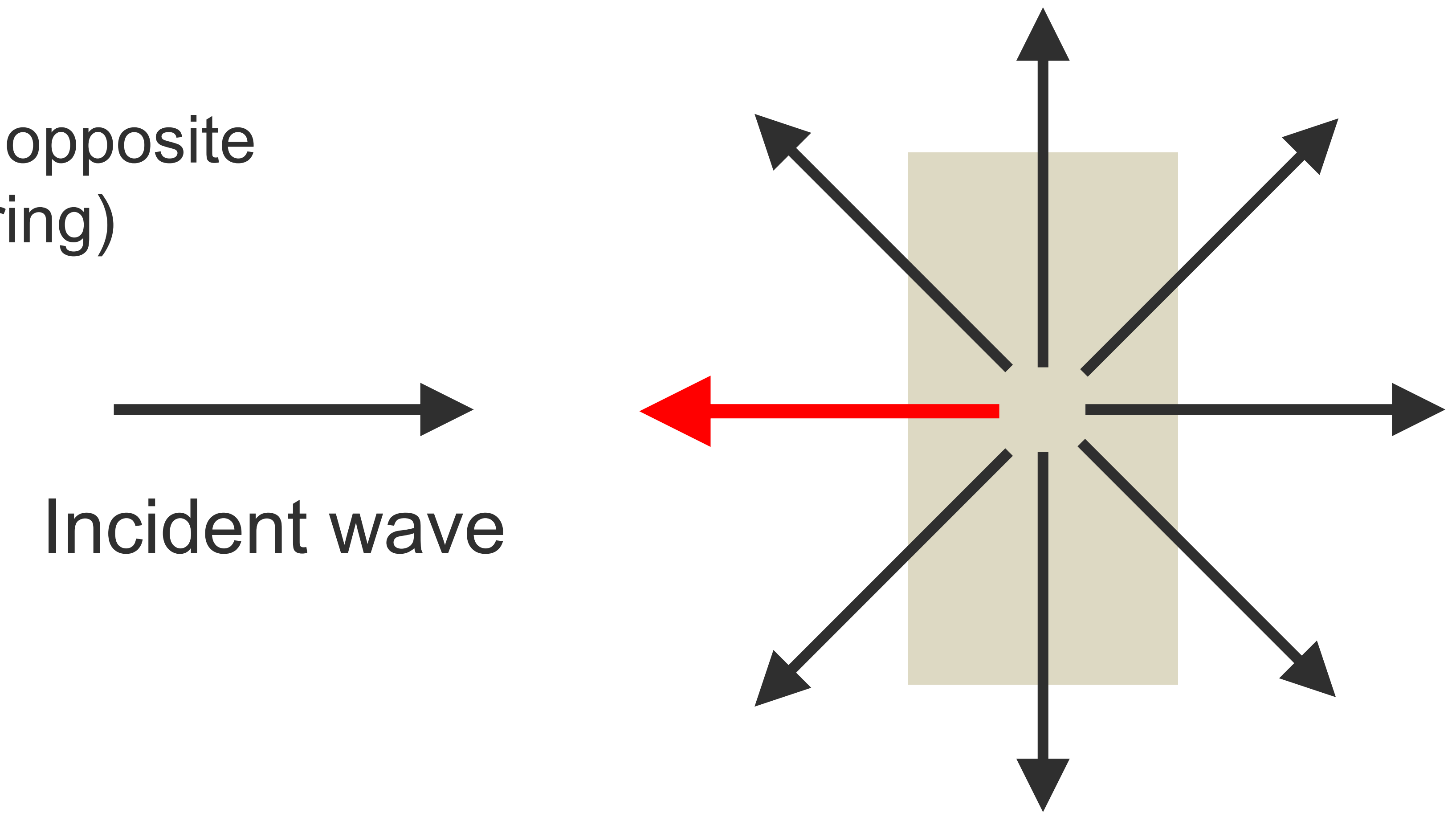

Origin of CBS

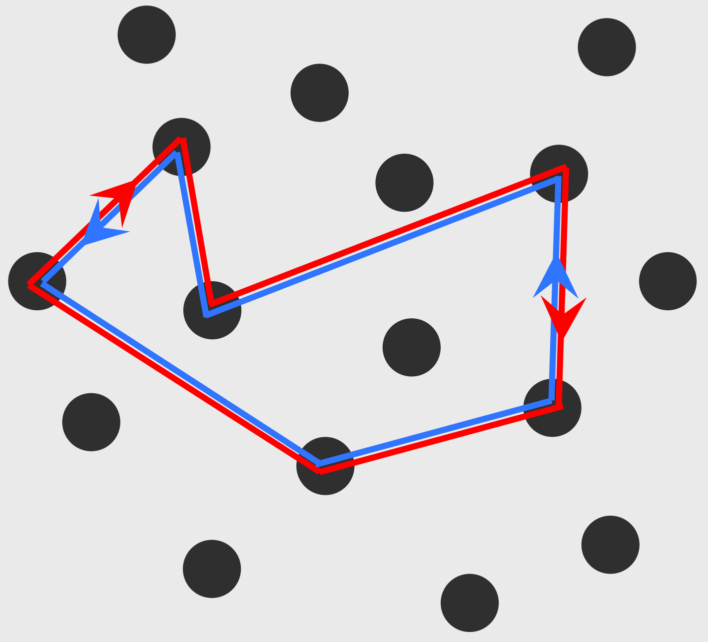

Reciprocal paths interfere constructively

→ "Weak localization"

phase difference = 0

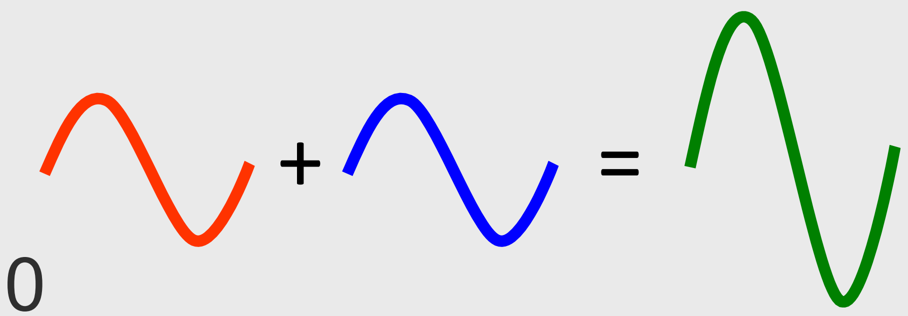

E. Akkermans and G. Montambaux, Mesoscopic Physics of Electrons and Photons (2007).
O. Sigwarth and C. Miniatura, AAPPS Bull. **32**, 23 (2022).

CBS in momentum space

Density distribution in $\boldsymbol{k}$-space

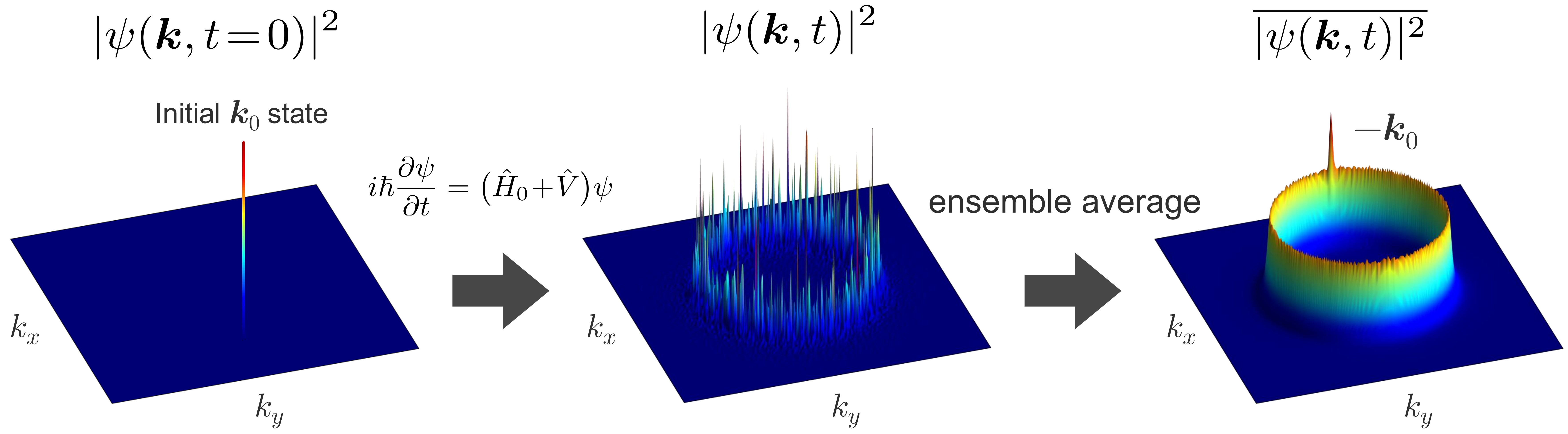

Plane wave $\boldsymbol{k}_0$ at $t = 0$ → Peak at $-\boldsymbol{k}_0$

Spin-orbit coupling (SOC)

	TRS[1]	SRS[2]
Orthogonal	○	○
Symplectic	○	×
Unitary	×	-

[1] time reversal symmetry [2] spin rotation symmetry

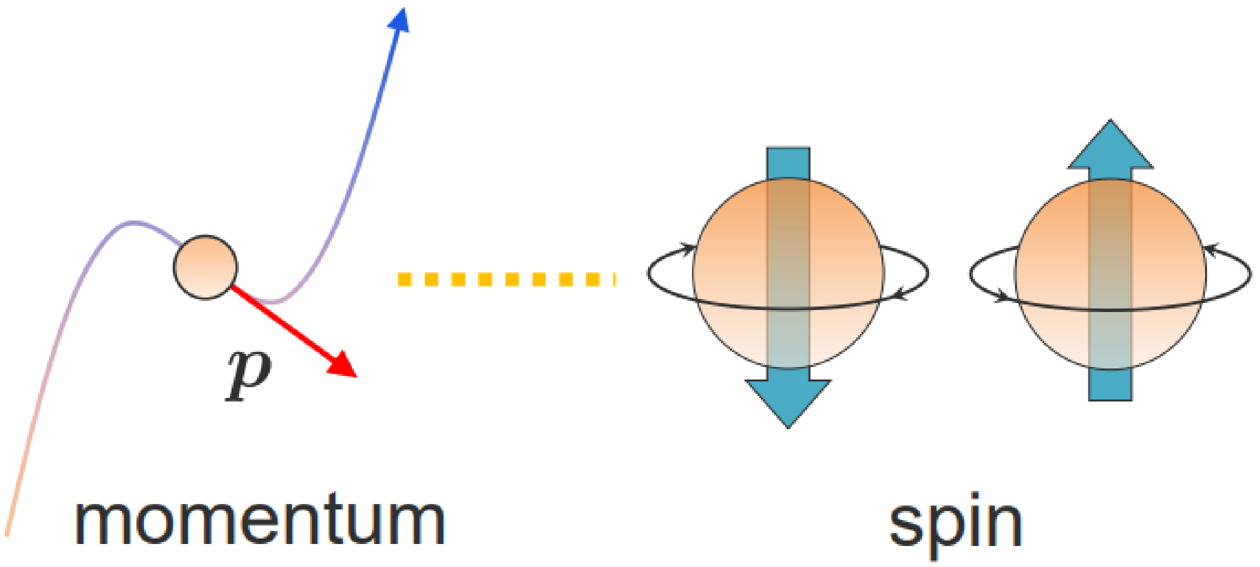

Weak SOC

Strong SOC

Constructive interference

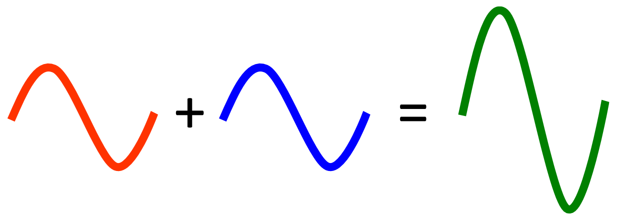

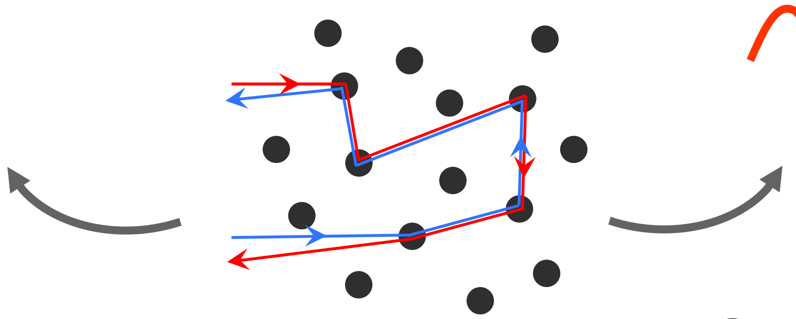

Destructive

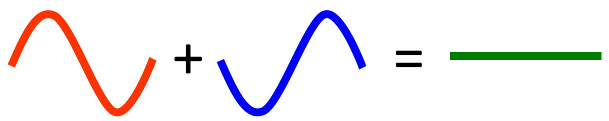

"Weak anti-localization"

S. Hikami *et al*., Prog. Theor. Phys. **63**, 707 (1980).

Spin independent disordered potential

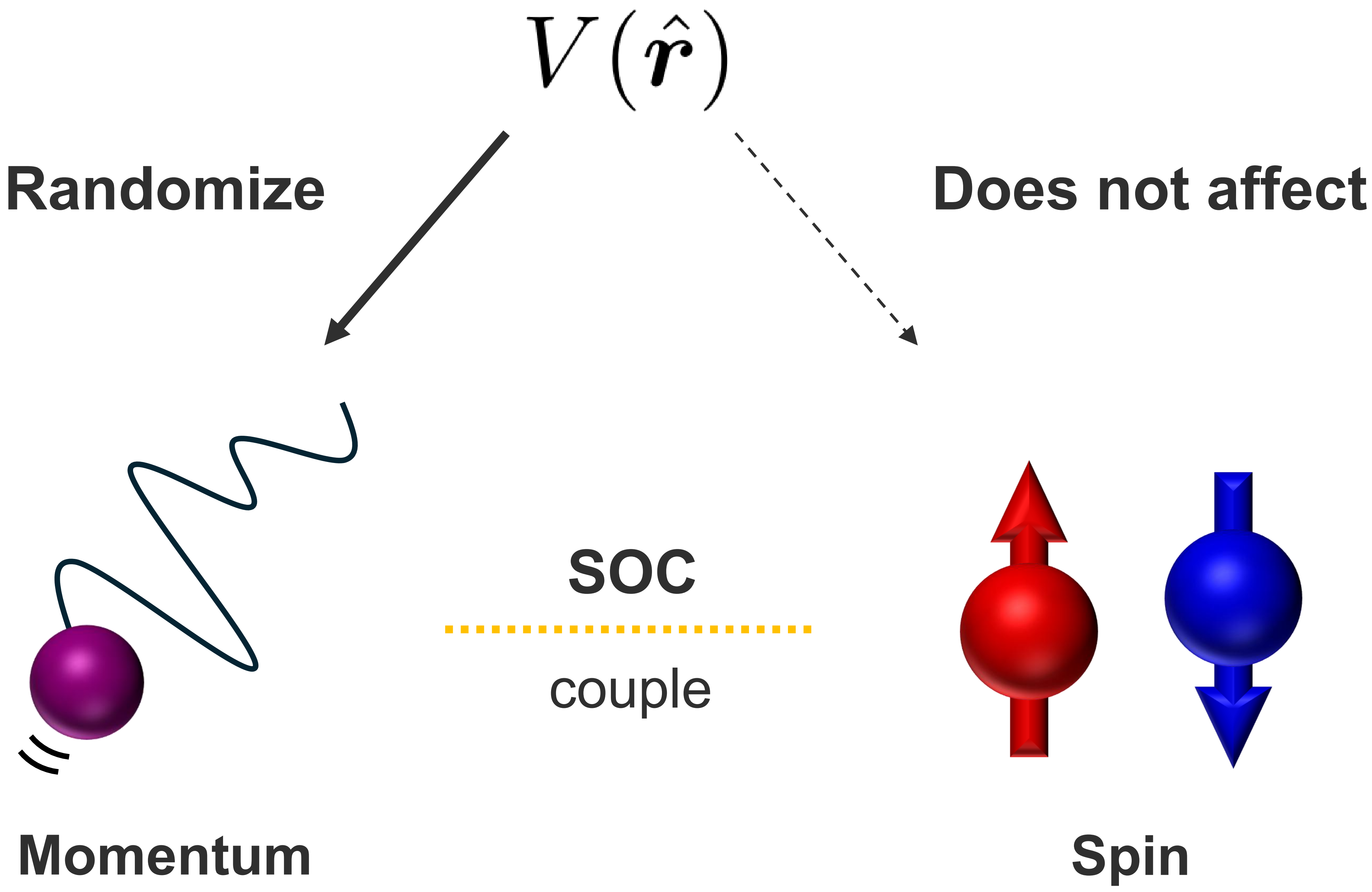

Disordered potentials make both momentum and spin dynamics nontrivial in the presence of SOC.

e.g. New timescale appears: MK and K. Slevin, PRA **109**, 033303 (2024)

General 2D Hamiltonian for spatially uniform SU(2) gauge field

SOC can be interpreted as an SU(2) gauge field

Hamiltonian for spin 1/2 particles confined in 2D plane
under general uniform SU(2) gauge fields

$$\hat{H}_0 = \frac{(\hat{\boldsymbol{p}} + \hat{\boldsymbol{A}})^2}{2m}$$ + spin-independent random potential term

where

$$\hat{\boldsymbol{A}} = M\hat{\boldsymbol{\sigma}}$$

$M \in \mathbb{R}^{2\times 3}$ and $\hat{\boldsymbol{\sigma}} = (\hat{\sigma}_1, \hat{\sigma}_2, \hat{\sigma}_3)$

"**Non-Abelian**"
vector potential

$$[\hat{A}_x, \hat{A}_y] \neq 0$$

Any spatially uniform SU(2) vector potential is expressed
by a linear combination of Pauli operators

General 2D Hamiltonian for spatially uniform SU(2) gauge field

$$\hat{H}_0 = \frac{(\hat{\boldsymbol{p}} + \hat{\boldsymbol{A}})^2}{2m}$$

$$\hat{\boldsymbol{A}} = M\hat{\boldsymbol{\sigma}}$$

$$M \in \mathbb{R}^{2\times 3}$$

6 parameters

$\Longleftrightarrow$

Equivalent after transformation of spatial and spin axes

See arXiv:2509.07312 for the proof

We use this form **without losing generality**

$$\begin{pmatrix} \hat{A}_x \\ \hat{A}_y \end{pmatrix} = \hbar\kappa \begin{pmatrix} \cos\eta\,\hat{\sigma}_x \\ \sin\eta\,\hat{\sigma}_y \end{pmatrix}$$

$$\kappa > 0, \quad \eta \in [0, \pi/4]$$

2 parameters

Example 1:
Rashba [1] **& Dresselhaus** [2] **SOC**

$$\eta = 0 \Leftrightarrow \text{R.=D.}^*, \quad \eta = \pi/4 \Leftrightarrow \text{pure R. or D.}$$

* This specific case was demonstrated in Ref. [3].

[1] Y. A. Bychkov and E. I. Rashba, J. Phys. C **17**, 6039 (1984).
[2] G. Dresselhaus, Phys. Rev. **100**, 580 (1955).
[3] B. A. Bernevig *et al.*, Phys. Rev. Lett. **97**, 236601 (2006).

Example 2:
Synthetic SOC in cold atoms

Tripod scheme [4,5]

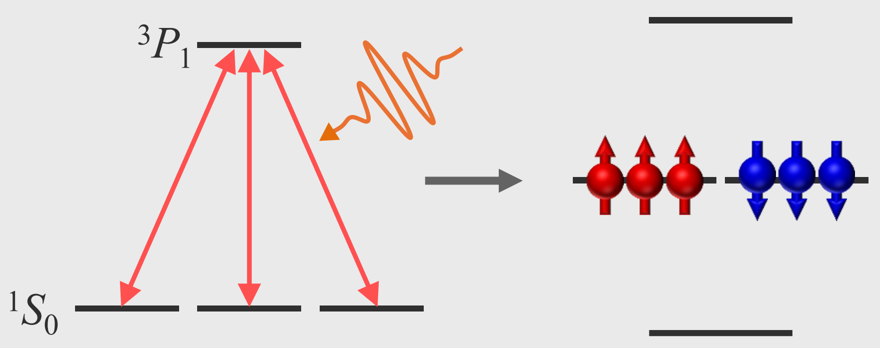

$$A_x = \frac{\hbar k_L}{2}\left(-\frac{\sqrt{3}}{3}\sigma_1 - \sigma_3 - 2 1_2\right)$$

$$A_y = \frac{\hbar k_L}{2}\left(\frac{\sqrt{3}}{3}\sigma_1 - \frac{1}{3}\sigma_3 - \frac{2}{3} 1_2\right)$$

suitable transformation

$$\eta = \frac{\pi}{6}$$

[4] F. Leroux *et al.*, Nat. Commun. **9**, 3580(2018).
[5] M. Hasan *et al.*, Phys. Rev. Lett. **129**, 130402 (2022).

Numerical simulation

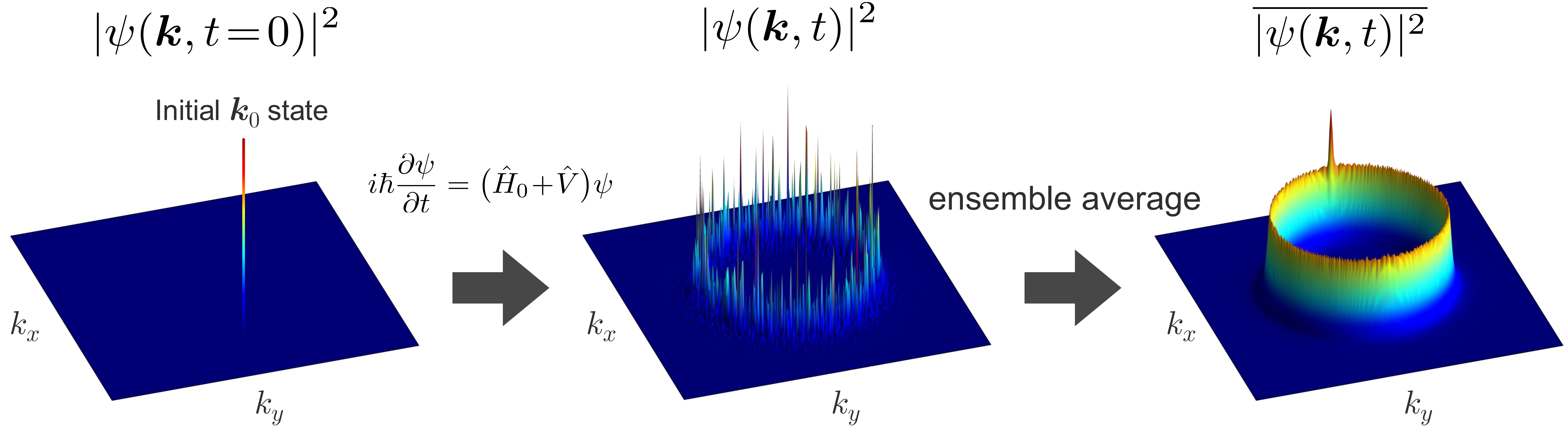

Plane wave at $t = 0 \rightarrow$ Time evolution by integrating Schrodinger eq.
$\rightarrow$ Repeat for many disorder realization and take average

Numerical simulation

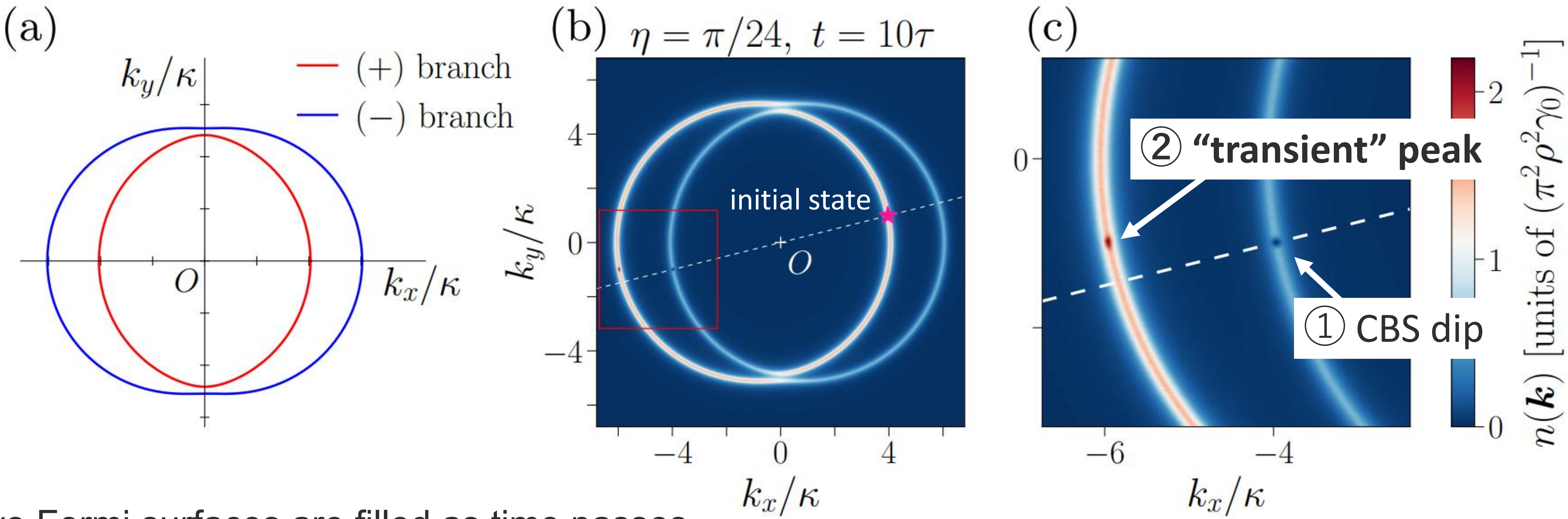

Two Fermi surfaces are filled as time passes

Coexistence of

① Robust CBS dip

② **Peak with finite lifetime at an offset from exact backscattering direction**

Condition of the simulation

$$\kappa\ell\eta \sim 1 \ll \kappa\ell < k_0\ell$$

ℓ: scattering mean free path

k_0: initial wave number

$$\begin{pmatrix}\hat{A}_x \\ \hat{A}_y\end{pmatrix} = \hbar\kappa\begin{pmatrix}\cos\eta\,\hat{\sigma}_x \\ \sin\eta\,\hat{\sigma}_y\end{pmatrix}$$

Non-Abelian gauge transformation

$$\hat{H}_0 = \frac{(\hat{\boldsymbol{p}} + \hat{\boldsymbol{A}})^2}{2m} \qquad \begin{pmatrix} \hat{A}_x \\ \hat{A}_y \end{pmatrix} = \hbar\kappa \begin{pmatrix} \cos\eta\,\hat{\sigma}_x \\ \sin\eta\,\hat{\sigma}_y \end{pmatrix} := \hbar \begin{pmatrix} \kappa_x\,\hat{\sigma}_x \\ \kappa_y\,\hat{\sigma}_y \end{pmatrix}$$

Gauge transformation

$$\hat{U} = e^{i\kappa_x \hat{x}\hat{\sigma}_1} = \cos\big(\kappa_x \hat{x}\big) + i\sin\big(\kappa_x \hat{x}\big)\hat{\sigma}_1$$

$$\psi \to \hat{U}\psi$$

$$\hat{A}_\mu \to \hat{A}'_\mu = \hat{U}\hat{A}_\mu\hat{U}^\dagger - i\,\hat{U}\partial_\mu\hat{U}^\dagger$$

(Does not affect the random potential)

$$\hat{U}\hat{H}_0\hat{U}^\dagger = \frac{(\hat{\boldsymbol{p}} + \hat{\boldsymbol{A}}')^2}{2m} = \frac{\hat{\boldsymbol{p}}^2}{2m} + \hat{H}_{\boldsymbol{A}} + \frac{(\hat{\boldsymbol{A}}')^2}{2m}$$

(constant)

$$\hat{A}_x \to \hat{A}'_x = 0$$

$$\hat{A}_y \to \hat{A}'_y = \hbar\kappa_y[\cos(2\kappa_x\hat{x})\hat{\sigma}_2 - \sin(2\kappa_y\hat{x})\hat{\sigma}_3]$$

where

$$\hat{H}_{\boldsymbol{A}} = \int \frac{d^2\boldsymbol{k}}{(2\pi)^2} \frac{\hbar^2\kappa_y k_y}{m} \,|\boldsymbol{k}+\boldsymbol{\kappa}_x, \rightarrow\rangle\,\langle\boldsymbol{k}-\boldsymbol{\kappa}_x, \leftarrow| + \mathrm{H.c.}$$

Spin-coupling term

$$|\rightarrow\rangle = \frac{|\uparrow\rangle + |\downarrow\rangle}{\sqrt{2}}, \quad |\leftarrow\rangle = \frac{|\uparrow\rangle - |\downarrow\rangle}{\sqrt{2}}$$

Momentum offset of the transient peak

$\eta \ll 1$ (Rashba ≈ Dresselhaus for example)

"New" frame $\boxed{\dfrac{\hat{\boldsymbol{p}}^2}{2m} + V(\hat{\boldsymbol{r}})} + \underbrace{\hat{H}_{\boldsymbol{A}}}_{\propto\, \eta}$

Same with the "spinless" Hamiltonian

→ Conventional CBS peak in the new frame

Dominant for the short-time dynamics

New frame

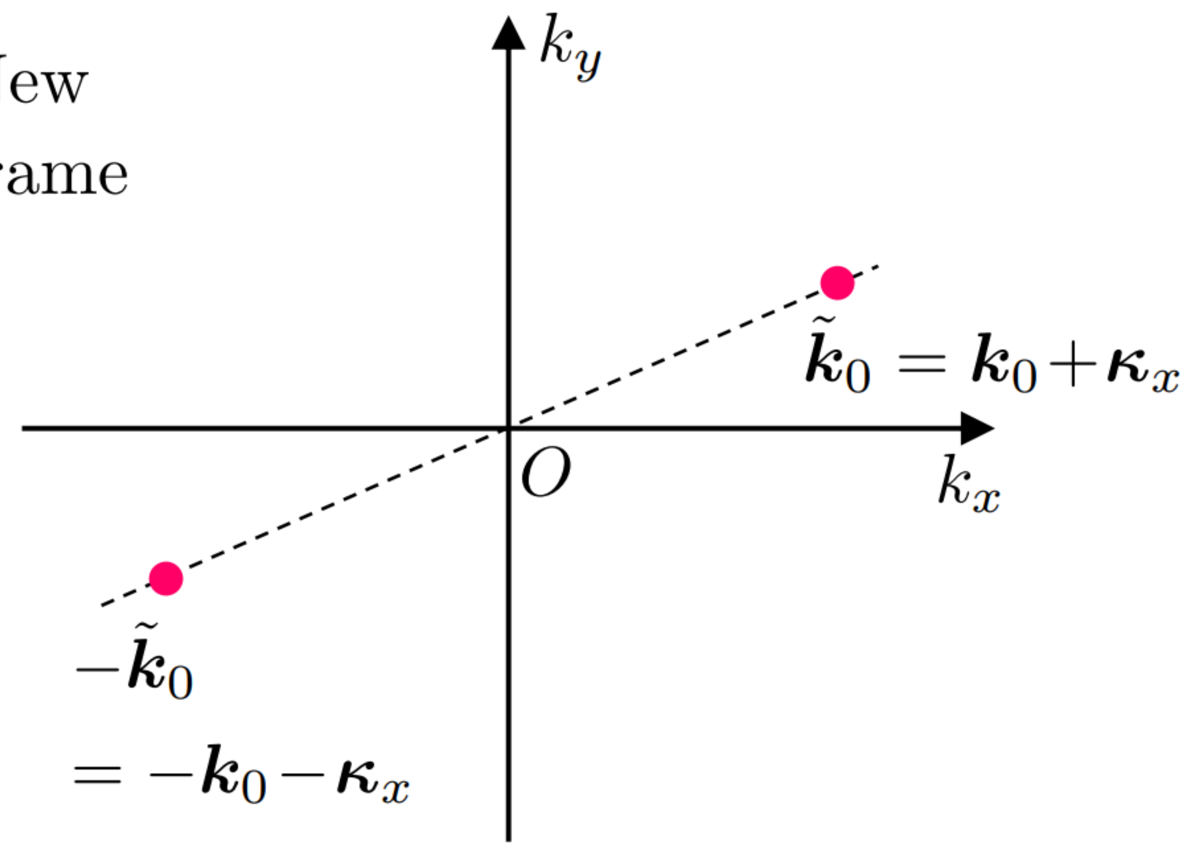

inverse transformation

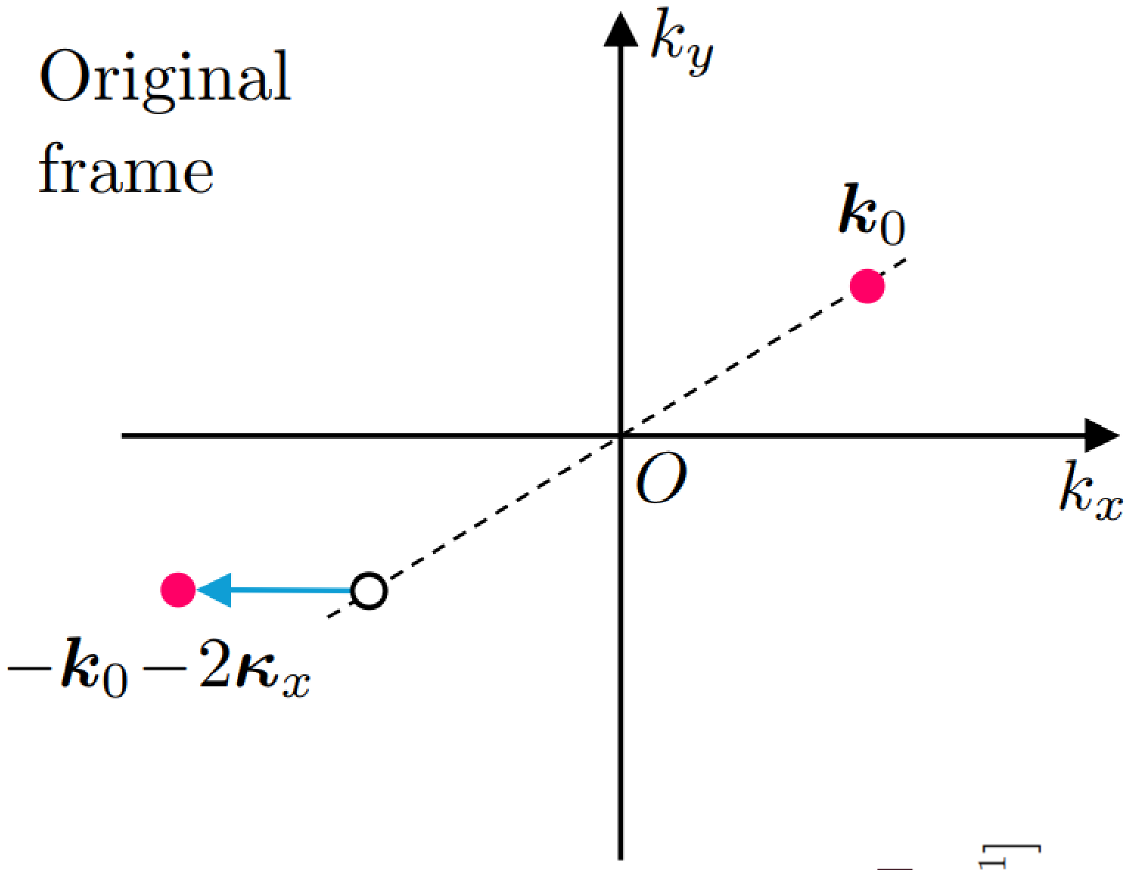

Note

$$\begin{pmatrix} \hat{A}_x \\ \hat{A}_y \end{pmatrix} = \hbar\kappa \begin{pmatrix} \cos\eta\,\hat{\sigma}_x \\ \sin\eta\,\hat{\sigma}_y \end{pmatrix} := \hbar \begin{pmatrix} \kappa_x\,\hat{\sigma}_x \\ \kappa_y\,\hat{\sigma}_y \end{pmatrix}$$

This picture is confirmed by simulation with small η

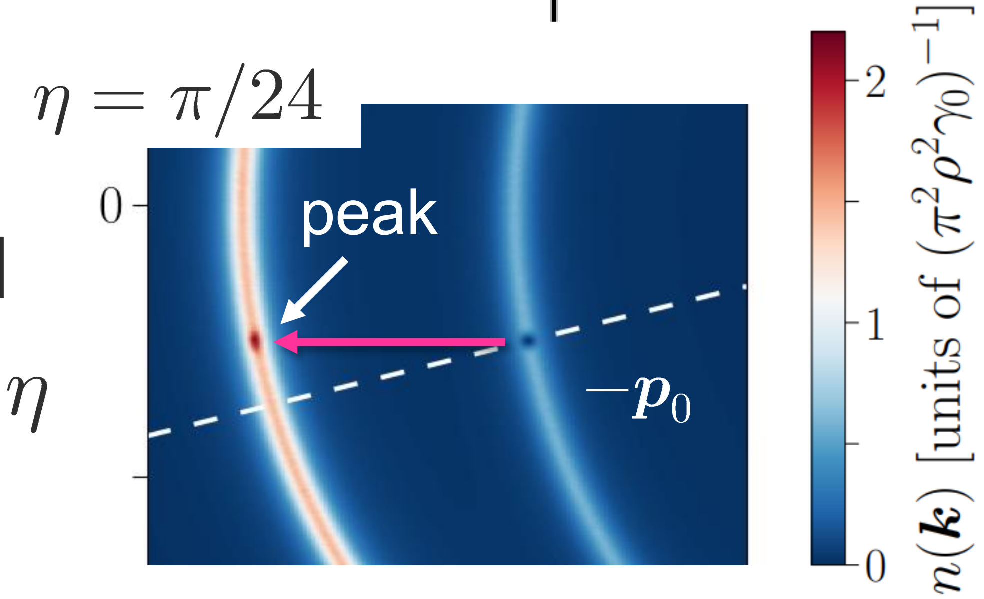

Analytic calculation for peak relaxation

Finite spin-coupling term H_A causes dephasing, leading to a finite lifetime (dephasing time) of the peak

Peak shape is analytically obtained by evaluating the maximally-crossed diagram series (Cooperon)

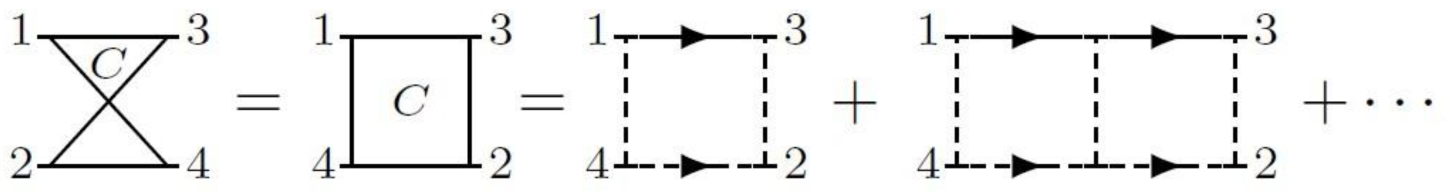

See Refs. [3,4] for how to treat time dependence

Peak shape at $t \gg \tau$ (scattering mean free time)

$$n^{\mathrm{C}}(\boldsymbol{k},t) = 2n_0\, e^{-Dt\,(\boldsymbol{k}+\boldsymbol{k_0}+2\boldsymbol{\kappa}_x)^2}\, e^{-t/\tau_\gamma}$$

Dephasing time

$$\tau_\gamma = \frac{\tau}{1-\gamma_0 \Pi^{\mathrm{C}}_{\rightarrow}(-2\boldsymbol{\kappa}_x, 0, E_0)}$$

where

$$\Pi^{\mathrm{C}}_{\rightarrow}(\boldsymbol{q},\omega,E) = \int \frac{d^2\boldsymbol{k}}{(2\pi)^2}\overline{G}_{\rightarrow}(\boldsymbol{k},E)\,\overline{G}^*_{\rightarrow}(\boldsymbol{q}-\boldsymbol{k},E-\hbar\omega)$$

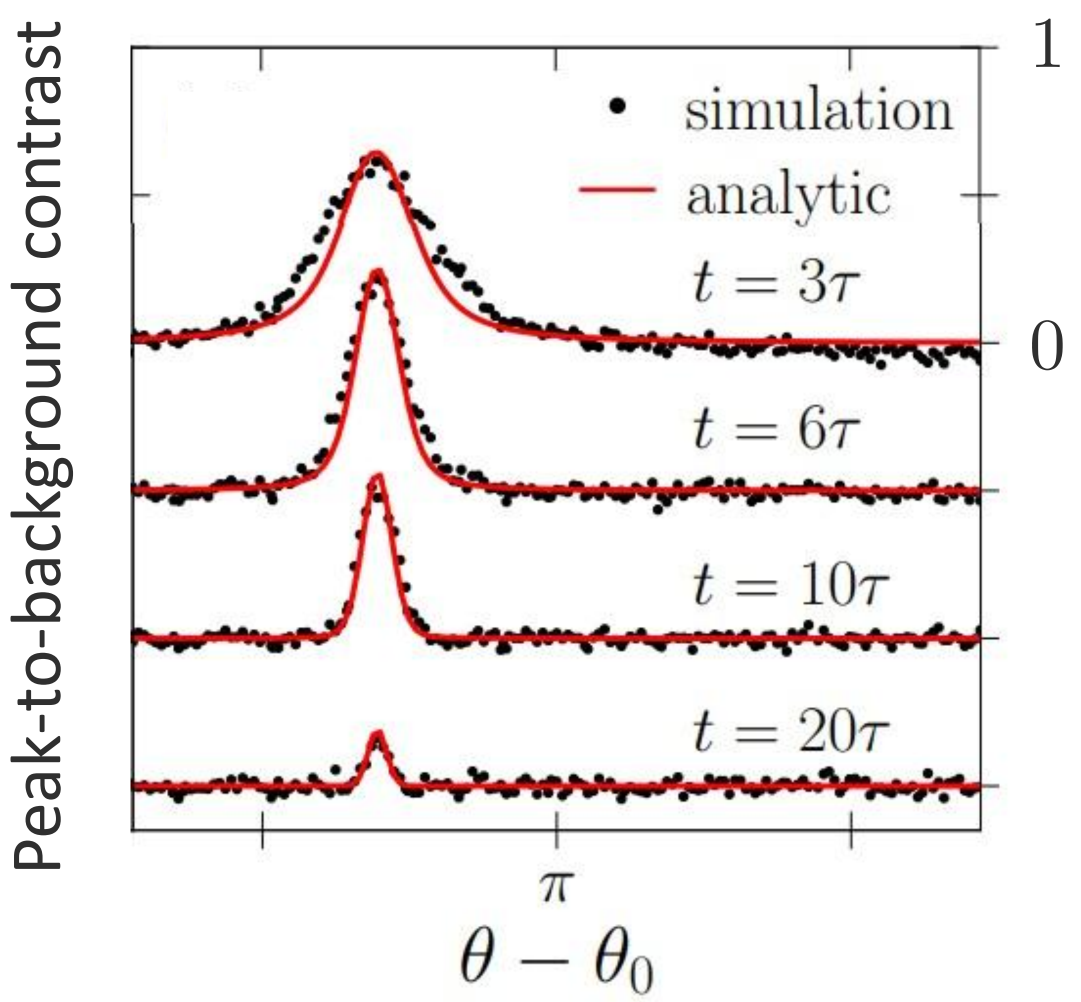

Analytic calculation reproduces well the simulation without any adjustable parameters

いま進めていること

密度演算子の不純物平均の摂動論を一般の形式でまとめている

$$
\begin{aligned}
\varrho_{\sigma\sigma'}(\boldsymbol{k},\boldsymbol{q},t) &= \overline{\left\langle \boldsymbol{k}+\frac{\boldsymbol{q}}{2},\sigma \middle| \psi(t) \right\rangle \left\langle \psi(t) \middle| \boldsymbol{k}-\frac{\boldsymbol{q}}{2},\sigma' \right\rangle} \\
&= \sum_{\mu,\nu} \int_{-\infty}^{\infty} \frac{d\omega}{2\pi} \int_{-\infty}^{\infty} \frac{dE}{2\pi} \int \frac{d^d\boldsymbol{k}'}{(2\pi)^d} e^{-i\omega t}\, \Phi_{\sigma\sigma',\mu\nu}(\boldsymbol{k},\boldsymbol{k}',\boldsymbol{q},E,\omega)\, \varrho_{\mu\nu}(\boldsymbol{k}',\boldsymbol{q},0)
\end{aligned}
$$

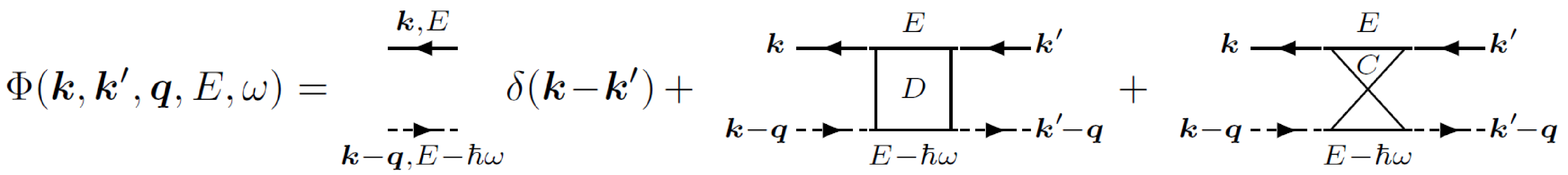

計算のルール

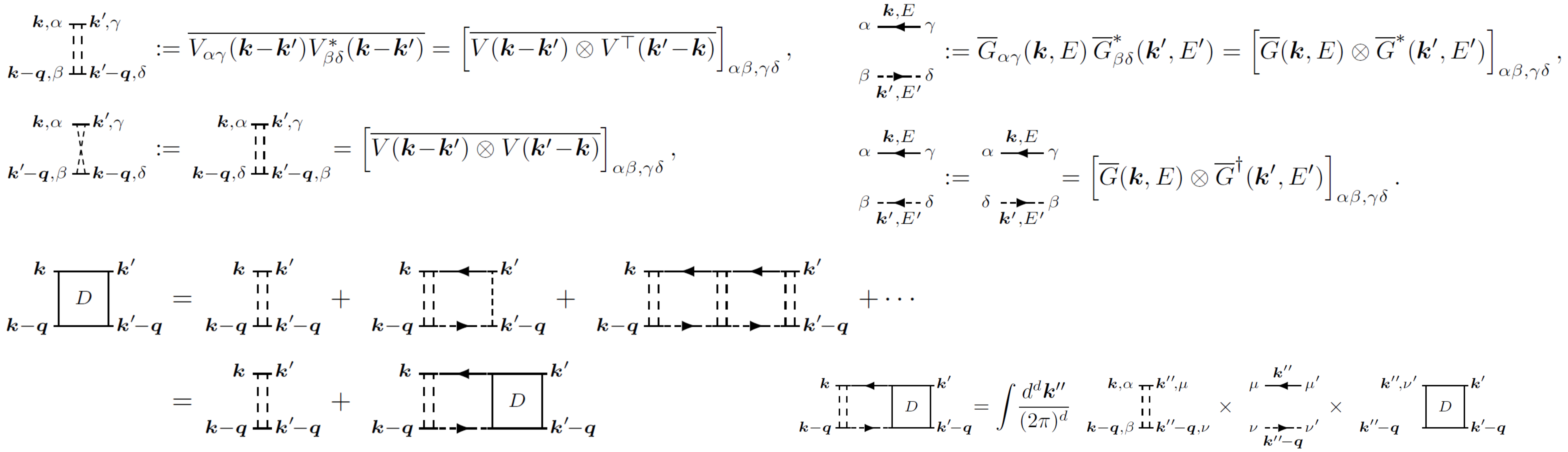

② 平坦バンドとディラック点を有する$\alpha - T_3$格子におけるカイラルd波超伝導

自発的時間反転対称性の破れをともなう超伝導

S. K. Ghosh *et al*., J. Phys.: Condens. Matter 33 (2021)

Table 2. A list of those strongly correlated SCs where μSR or the Kerr effect have been used to provide evidence for either the presence or absence of TRS in the superconducting state.

Material	Broken TRS?	Reference
UPt_3	✓/×	[22, 38, 44]
UBe_{13}	×	[32]
$U_{1-x}Th_xBe_{13}$ $(0.02 \leqslant x \leqslant 0.04)$	✓	[32]
URu_2Si_2	✓	[23]
UTe_2	✓	[41]
$CeCu_2Si_2$	×	[45]
$CeCoIn_5$	×	[46]
$CeIrIn_5$	×	[46]
$YBa_2Cu_3O_7$	×	[47, 48]
$Bi_2Sr_{2-x}La_xCuO_{6+\delta}$	×	[47, 49]
$Ba_{1-x}K_xFe_2As_2$	×, ✓ $(0.7 \lesssim x \lesssim 0.85)$	[50–52]
Sr_2RuO_4	✓	[21, 33]
$Pr(Os_{1-x}Ru_x)_4Sb_{12}$	✓	[53, 54]
$Pr_{1-y}La_yOs_4Sb_{12}$ $(y < 1)$	✓	[54]
$Pr_{1-y}La_yPt_4Ge_{12}$ $(y < 1)$	✓	[55, 56]

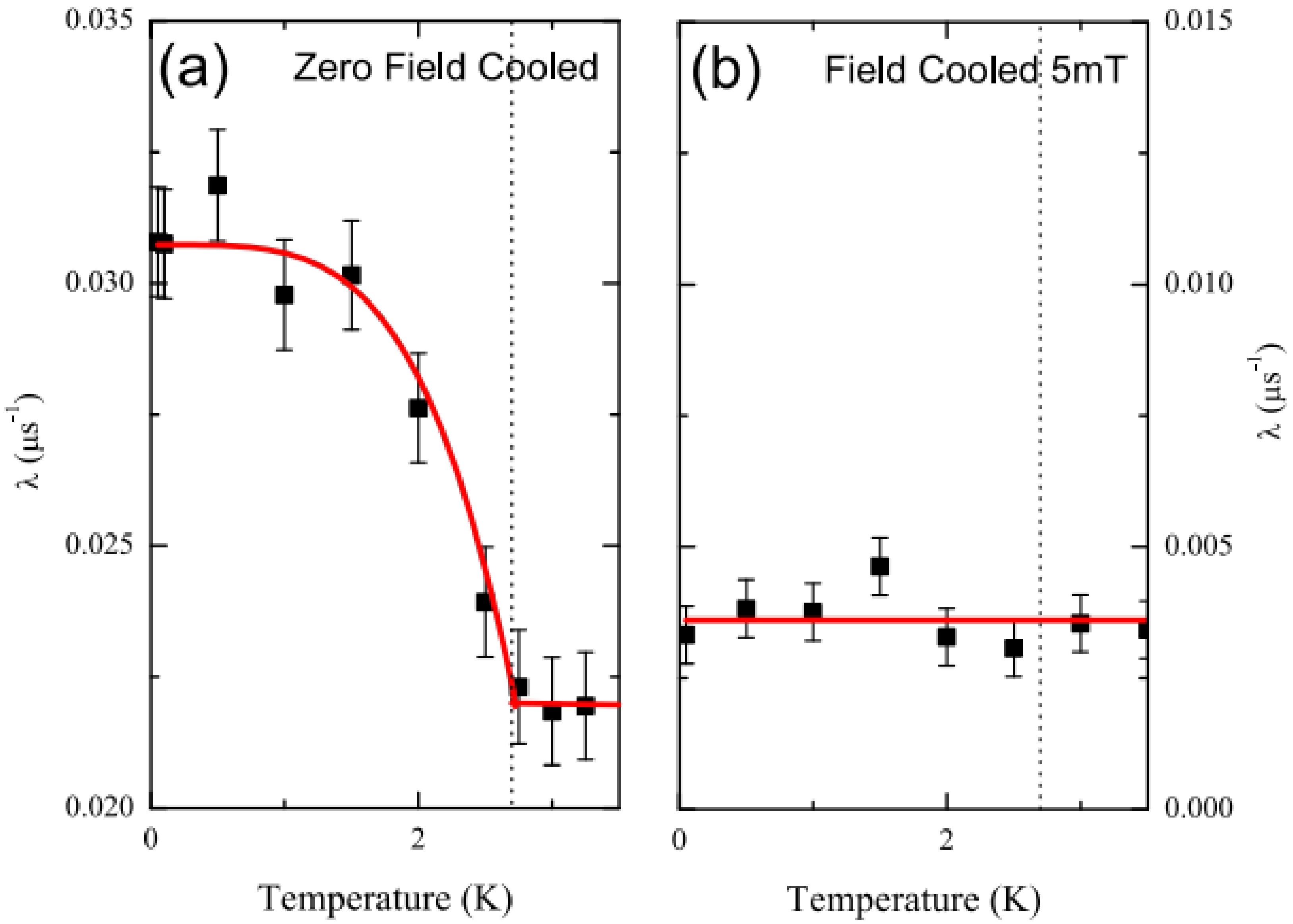

Lorentzian relaxation rate λ_{ZF} obtained from fitting μSR spectra of $LaNiC_2$ in (a) zero-field, and (b) a longitudinal field of 5 mT.

α-T_3模型

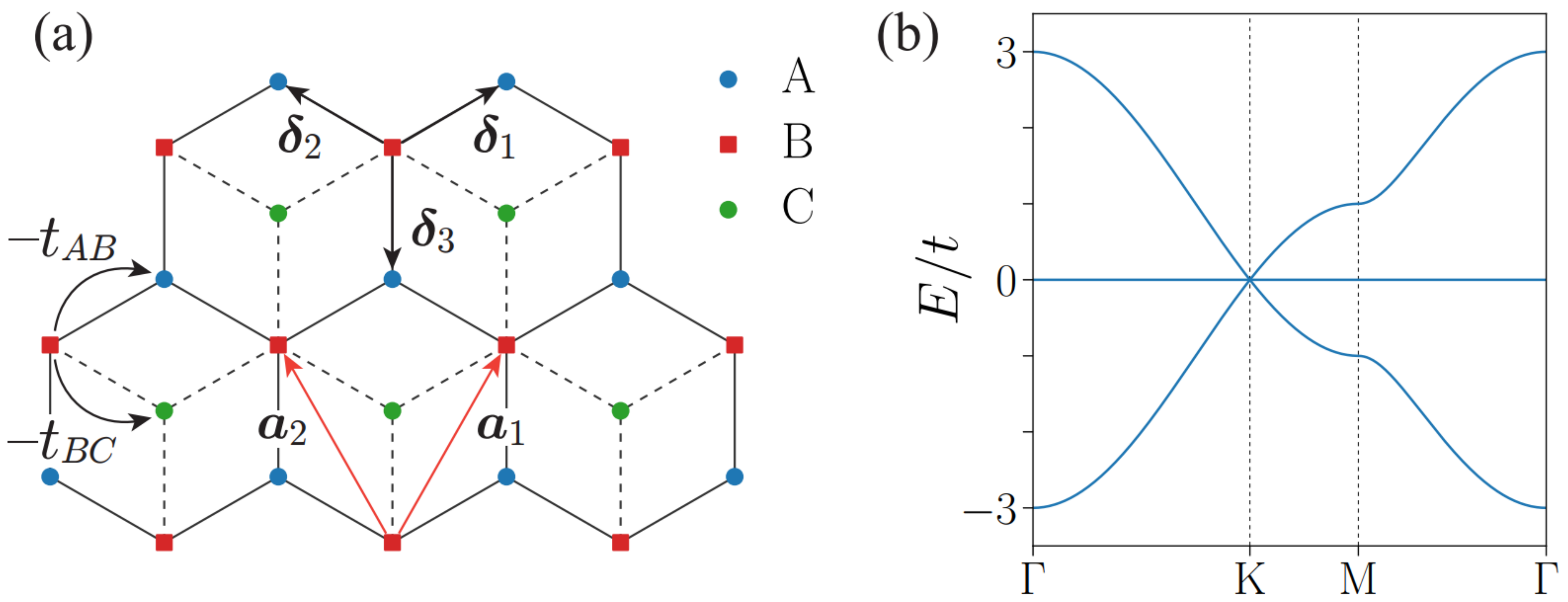

$$t_{ij} = \begin{cases} t_{AB} = t\cos\varphi, & \text{A-B nearest neighber,} \\ t_{BC} = t\sin\varphi, & \text{B-C nearest neighber,} \\ 0, & \text{otherwise.} \end{cases}$$

$$H_0(\boldsymbol{k}) = \begin{pmatrix} 0 & f(\boldsymbol{k})\cos\varphi & 0 \\ f^*(\boldsymbol{k})\cos\varphi & 0 & f(\boldsymbol{k})\sin\varphi \\ 0 & f^*(\boldsymbol{k})\sin\varphi & 0 \end{pmatrix} \qquad f(\boldsymbol{k}) = -t\sum_{\ell=1}^{3} e^{i\boldsymbol{k}\cdot\boldsymbol{\delta}_\ell}$$

α-T_3模型

K(K')点を囲む経路に対するBerry位相

$\gamma = \pm\pi$　　$\gamma = \pm\pi\cos 2\varphi$　(分散バンド)　　$\gamma = 0$

$\alpha = 0$
"Graphene"

$\alpha = 1$
"Dice model"

ホッピングの比が変わると
固有状態は変化・バンドは不変

固有ベクトル

$$|\boldsymbol{k}, \pm\rangle = \frac{1}{\sqrt{2}}\begin{pmatrix} e^{i\theta(\boldsymbol{k})}\cos\varphi \\ \pm 1 \\ e^{-i\theta(\boldsymbol{k})}\sin\varphi \end{pmatrix}, \ |\boldsymbol{k}, 0\rangle = \begin{pmatrix} e^{-i\theta(\boldsymbol{k})}\sin\varphi \\ 0 \\ -e^{i\theta(\boldsymbol{k})}\cos\varphi \end{pmatrix}$$

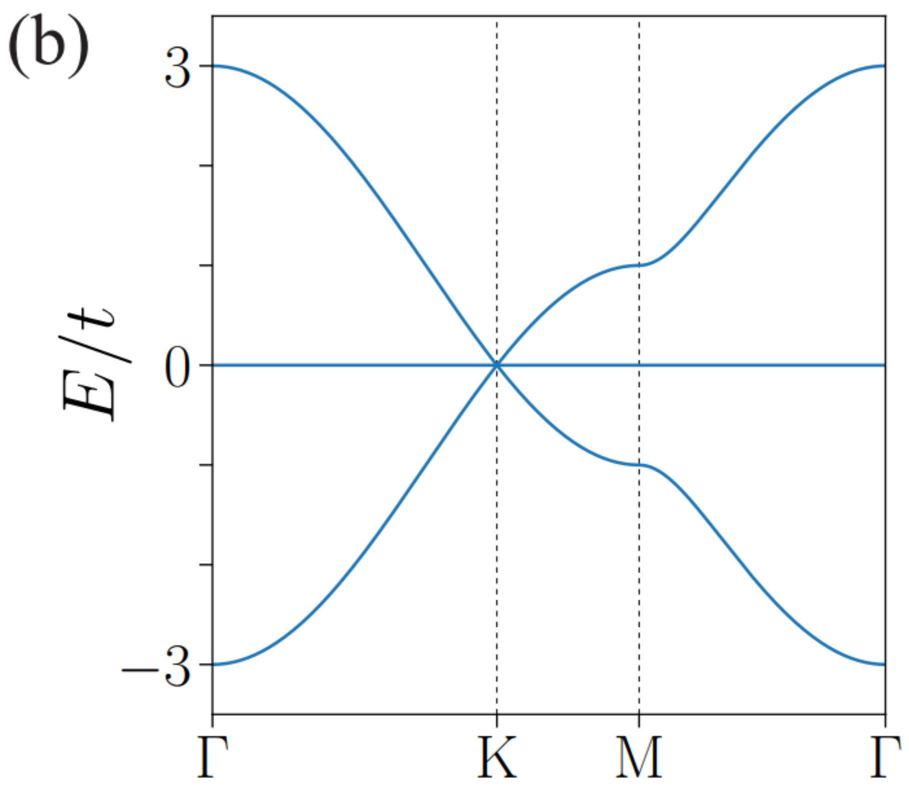

Hubbard模型の揺らぎ交換(FLEX)近似+線形化Eliashberg方程式

Fluctuation exchange (FLEX) approximation [1]

Dyson eq.

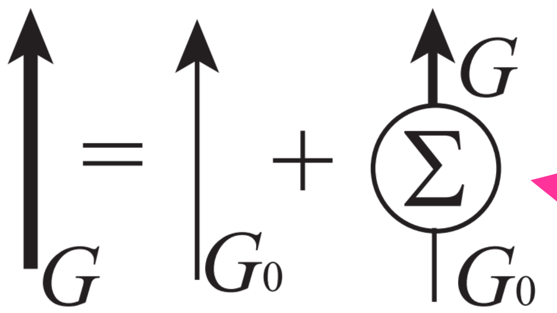

Self-energy

"feedback"

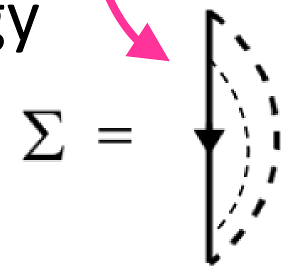

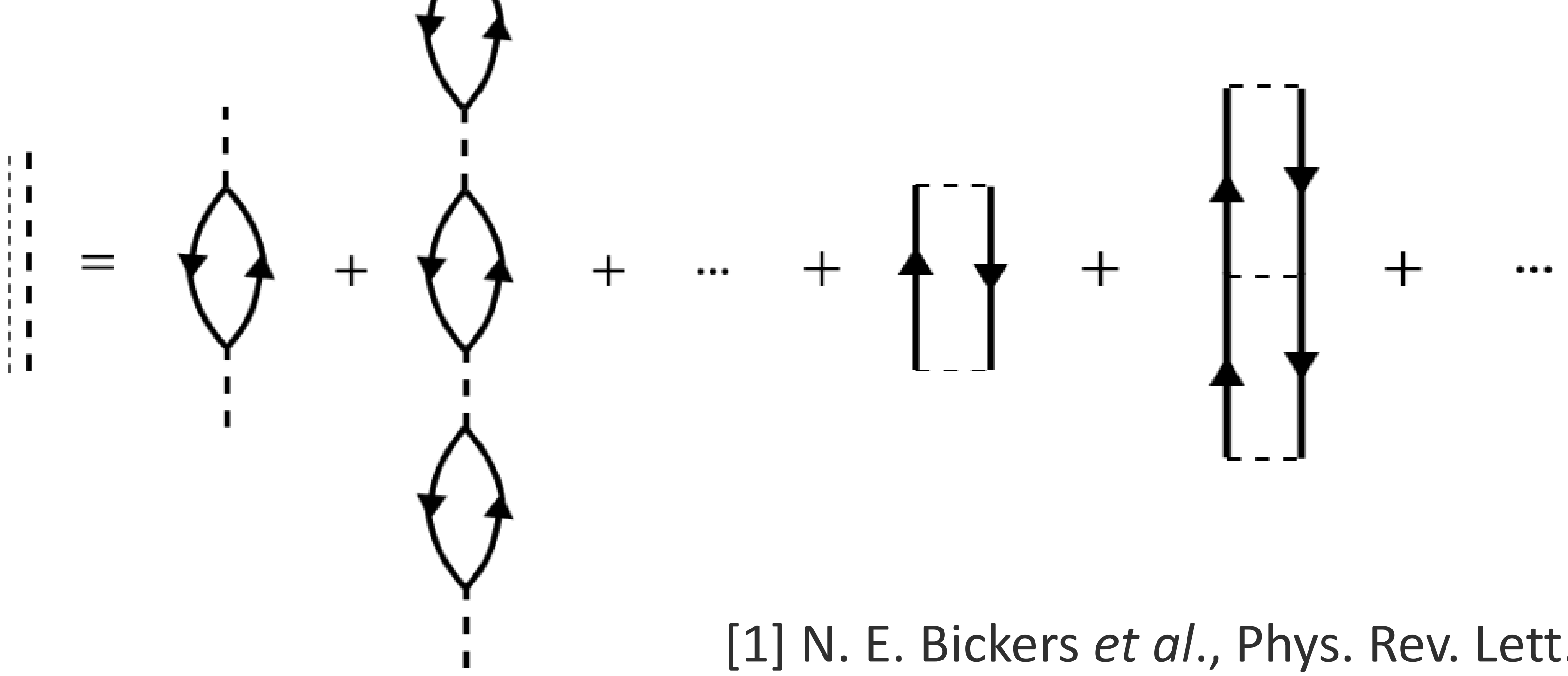

Linearlized Eliashberg equation

Anormalous self-energy
(Gap function)

Pairing interaction

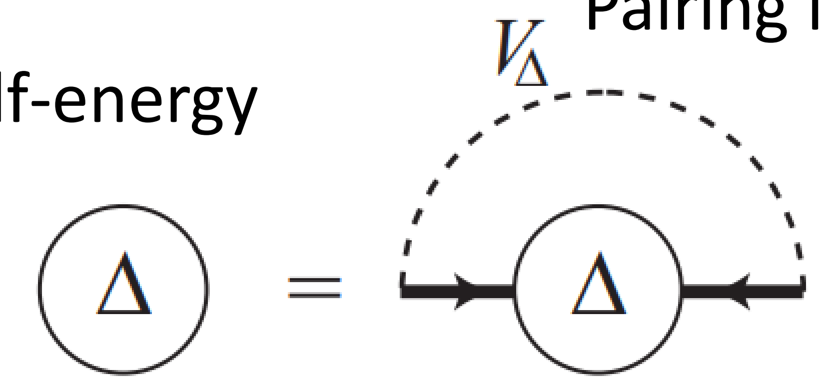

$(T = T_c)$

⇕

Eigenvalue problem

$$\lambda\Delta = A\Delta \qquad \lambda = 1 \text{ at } T = T_c$$

Larger λ ⟷ Higer T_c (assumption)

[1] N. E. Bickers *et al.*, Phys. Rev. Lett. **62**, 961 (1989)

線形化Eliashberg方程式の固有値 λ

Condition

$$\frac{U}{t} = 4 \qquad \frac{T}{t} = 0.002$$

W: band width

$(N_x, N_y) = (48, 48)$,
$N_\omega = 4098 \times 2$

Non-interacting

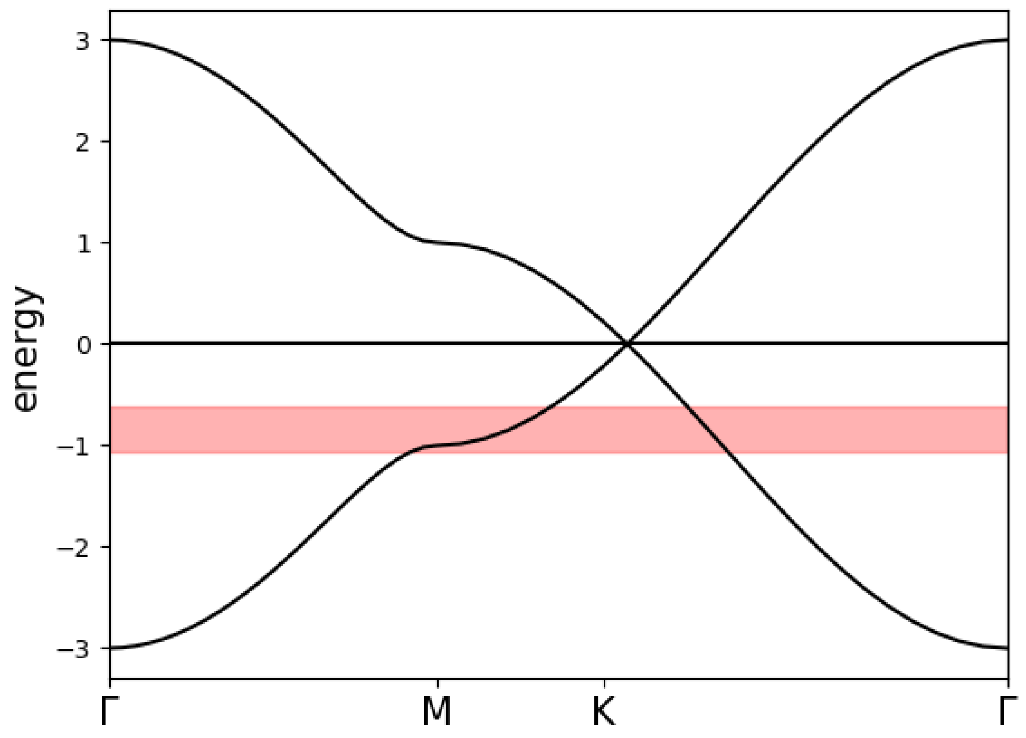

chem. pot.

Gap symmetry: ***d*-wave** (discuss later)

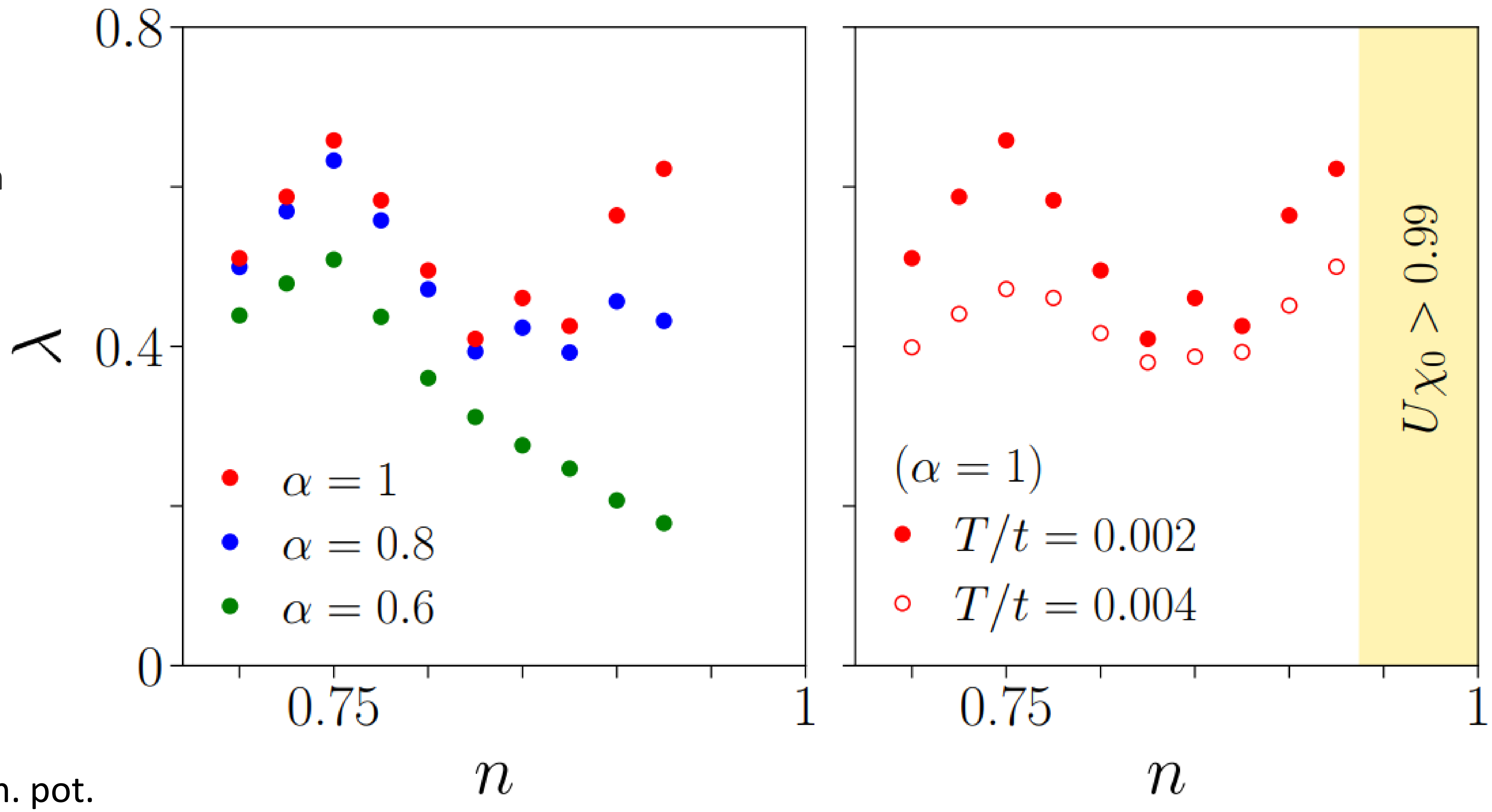

FLEX+線形化Eliashberg の異常自己エネルギー（ギャップ関数）

$\alpha = 1, n = 0.9$

$\Delta_{xy}(\boldsymbol{k})$ $\Delta_{x^2-y^2}(\boldsymbol{k})$

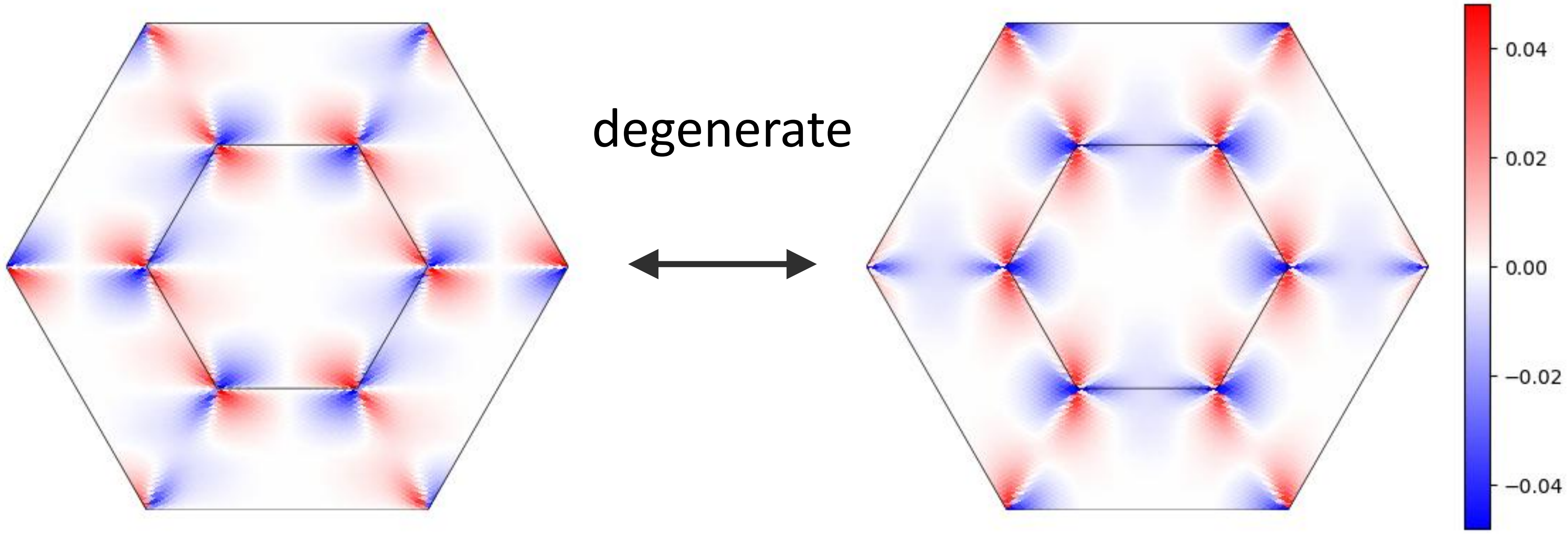

FLEX+線形化Eliashberg の異常自己エネルギー（ギャップ関数）

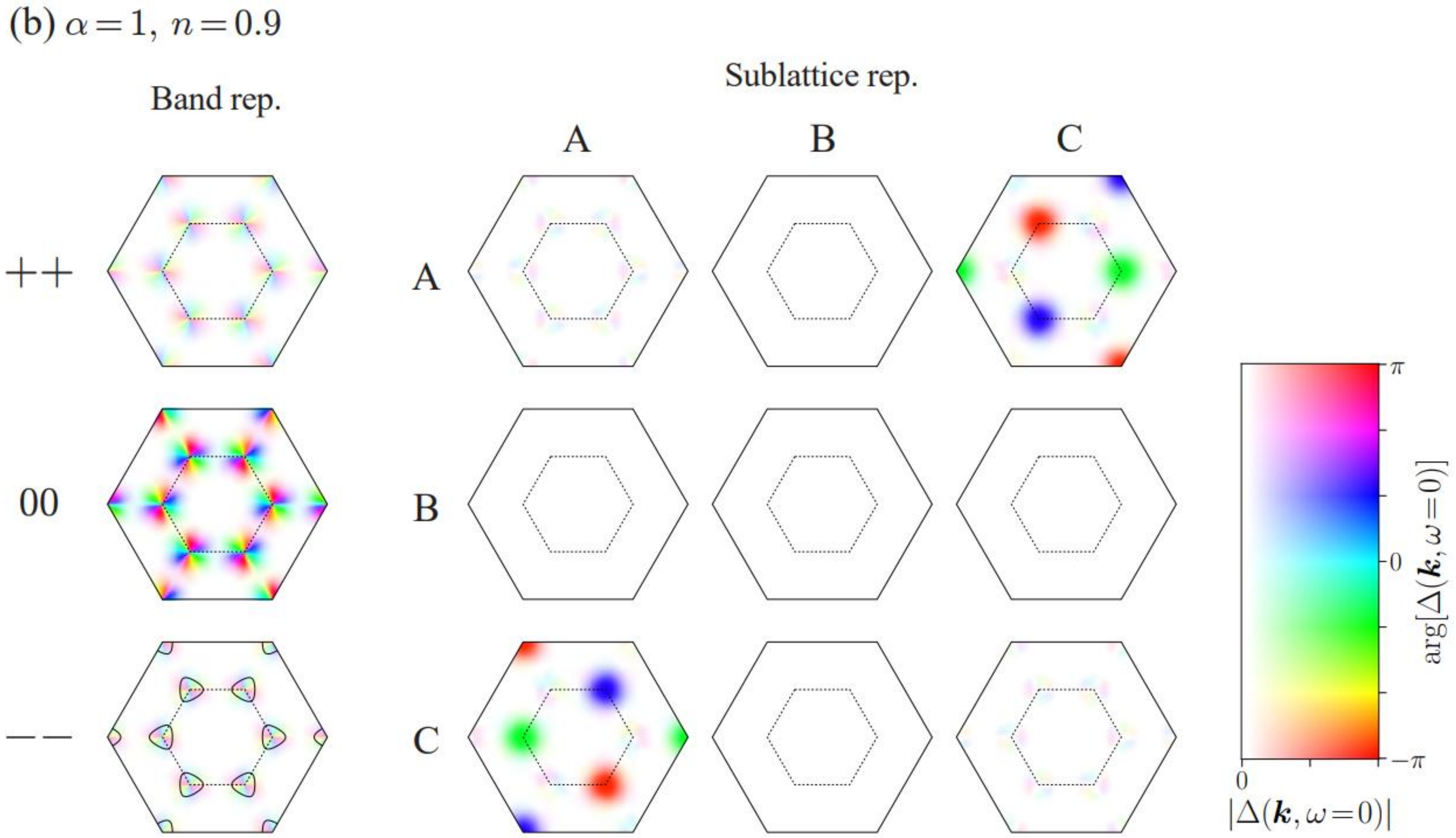

FLEX+線形化Eliashberg の異常自己エネルギー（ギャップ関数）

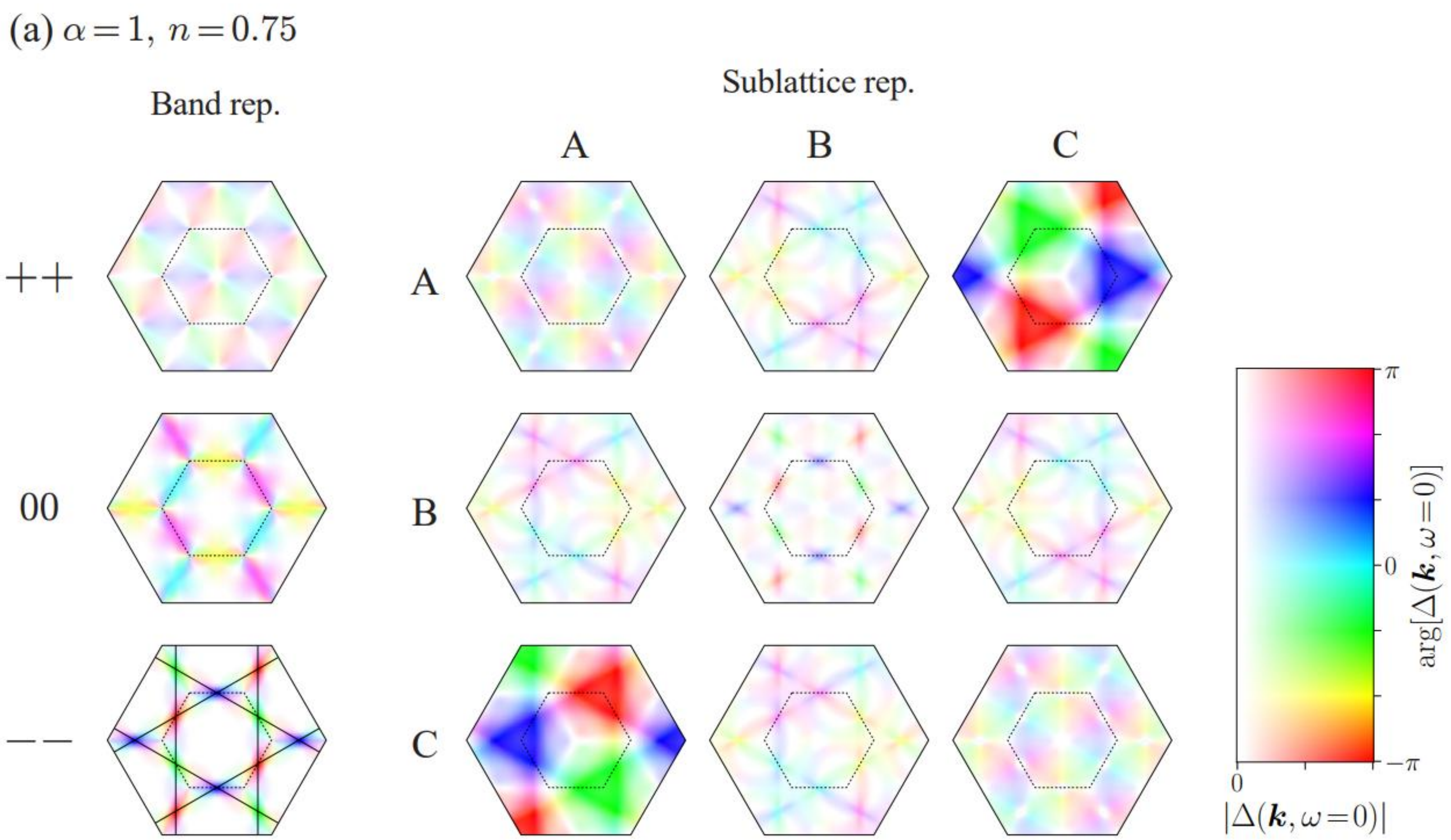

有効模型の平均場解析

最近接サイト間に引力相互作用を加えた
拡張ハバード模型

$$\hat{H}^{\mathrm{eff}}_{\mathrm{int}} = U\sum_{i} \hat{n}_{i,\uparrow}\hat{n}_{j,\downarrow} + \frac{1}{2}\sum_{\langle i,j\rangle,\sigma,\sigma'} V_{ij}\,\hat{n}_{i,\sigma}\hat{n}_{j,\sigma'}$$

$$V_{ij} = \begin{cases} -V_{\mathrm{AB}}, & \text{A–B nearest neighbors,} \\ -V_{\mathrm{BC}}, & \text{B–C nearest neighbors,} \\ -V_{\mathrm{CA}}, & \text{C–A nearest neighbors.} \end{cases}$$

$$\hat{H}^{\mathrm{eff}}_{\mathrm{int}} = \sum_{\boldsymbol{k},\boldsymbol{k}',\alpha,\beta} V_{\alpha\beta}(\boldsymbol{k}-\boldsymbol{k}')\,\hat{c}^{\dagger}_{\boldsymbol{k},\uparrow,\alpha}\hat{c}^{\dagger}_{-\boldsymbol{k},\downarrow,\beta}\hat{c}_{-\boldsymbol{k}',\downarrow,\beta}\hat{c}_{\boldsymbol{k}',\uparrow,\alpha}$$

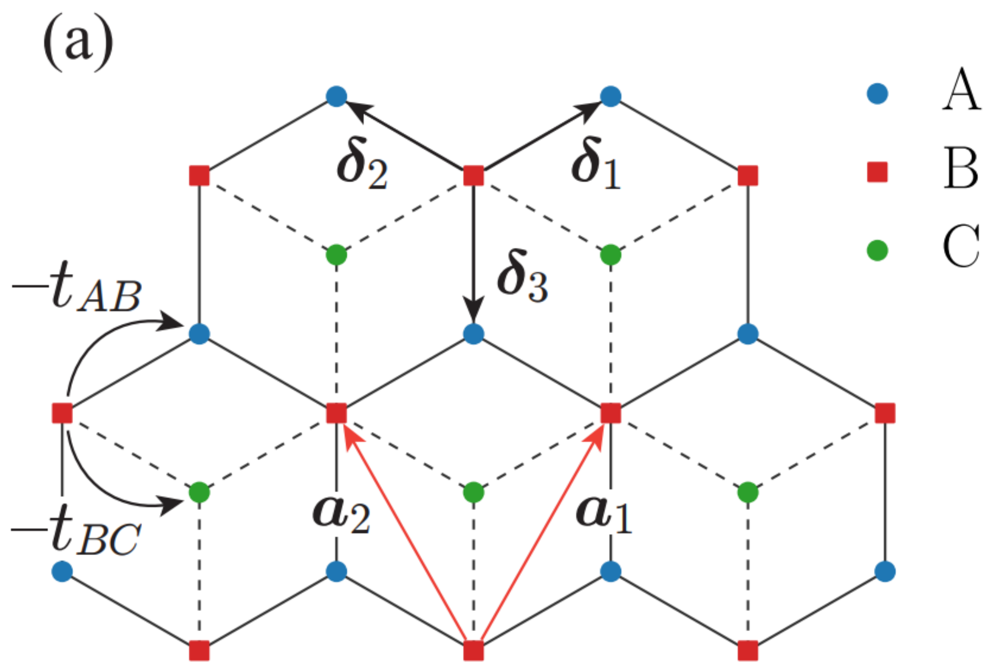

$$V_{\alpha\beta}(\boldsymbol{k}) = \begin{cases} U, & \alpha=\beta, \\ -V_{\alpha\beta}f(\boldsymbol{k}), & \alpha\beta = \text{AB, BC, CA,} \\ -V_{\alpha\beta}f^{*}(\boldsymbol{k}), & \alpha\beta = \text{BA, CB, AC.} \end{cases}$$

$$f(\boldsymbol{k}) = -t\sum_{\ell=1}^{3} e^{i\boldsymbol{k}\cdot\boldsymbol{\delta}_\ell}$$

有効模型の平均場解析

平均場ハミルトニアン　$c^\dagger c^\dagger c c \approx \langle c^\dagger c^\dagger \rangle c c + c^\dagger c^\dagger \langle c c \rangle$

$$H_{\mathrm{BdG}}(\boldsymbol{k}) = \begin{pmatrix} H_0(\boldsymbol{k}) - \mu \mathbb{1} & \Delta(\boldsymbol{k}) \\ \Delta^\dagger(\boldsymbol{k}) & -H_0^\top(-\boldsymbol{k}) + \mu \mathbb{1} \end{pmatrix}$$

$$\Delta_{\alpha\beta}(\boldsymbol{k}) = -\sum_{\boldsymbol{k}'} V_{\alpha\beta}(\boldsymbol{k}-\boldsymbol{k}') \langle c_{\boldsymbol{k}',\uparrow,\alpha}\, c_{-\boldsymbol{k}',\downarrow,\beta} \rangle$$

自己無撞着に解く

eigenvalues E_n and eigenvectors $\boldsymbol{\phi}_{\boldsymbol{k}}^{(n)} = (\boldsymbol{u}_{\boldsymbol{k}}^{(n)}, \boldsymbol{v}_{\boldsymbol{k}}^{(n)})$

$$\Delta_{\alpha\beta}(\boldsymbol{k}) = -\sum_{\boldsymbol{k}'} V_{\alpha\beta}(\boldsymbol{k}-\boldsymbol{k}') \sum_{n,\, E_n>0} u_{\boldsymbol{k},\alpha}^{(n)} v_{\boldsymbol{k},\beta}^{(n)*} \tanh \frac{\beta E_n}{2}$$

有効模型の平均場解析

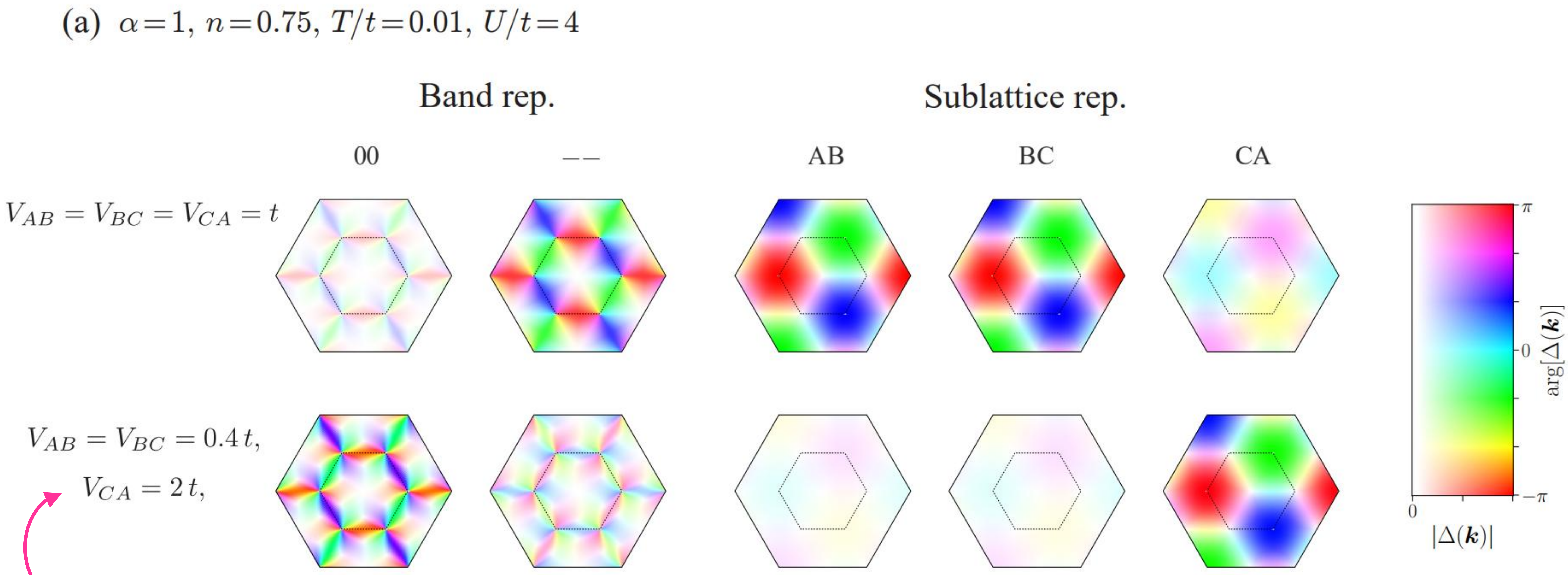

FLEX+線形化Eliashberg と整合

トポロジカル絶縁体・超伝導体の分類表

Altland-Zirnbauer class

時間反転　粒子正孔　カイラル

		TRS	PHS	SLS	$d=1$	$d=2$	$d=3$
Standard	A (unitary)	0	0	0	-	$\mathbb{Z}$	-
(Wigner-Dyson)	AI (orthogonal)	+1	0	0	-	-	-
	AII (symplectic)	−1	0	0	-	$\mathbb{Z}_2$	$\mathbb{Z}_2$
Chiral	AIII (chiral unitary)	0	0	1	$\mathbb{Z}$	-	$\mathbb{Z}$
(sublattice)	BDI (chiral orthogonal)	+1	+1	1	$\mathbb{Z}$	-	-
	CII (chiral symplectic)	−1	−1	1	$\mathbb{Z}$	-	$\mathbb{Z}_2$
BdG	D	0	+1	0	$\mathbb{Z}_2$	$\mathbb{Z}$	-
	C	0	−1	0	-	$\mathbb{Z}$	-
	DIII	−1	+1	1	$\mathbb{Z}_2$	$\mathbb{Z}_2$	$\mathbb{Z}$
	CI	+1	−1	1	-	-	$\mathbb{Z}$

A. P. Schnyder, Phys. Rev. B **78**, 195125 (2008)

整数のトポロジカル数で特徴づけられるトポロジカル相が在り得る

有効模型の平均場解析

未解決：チャーン数の符号

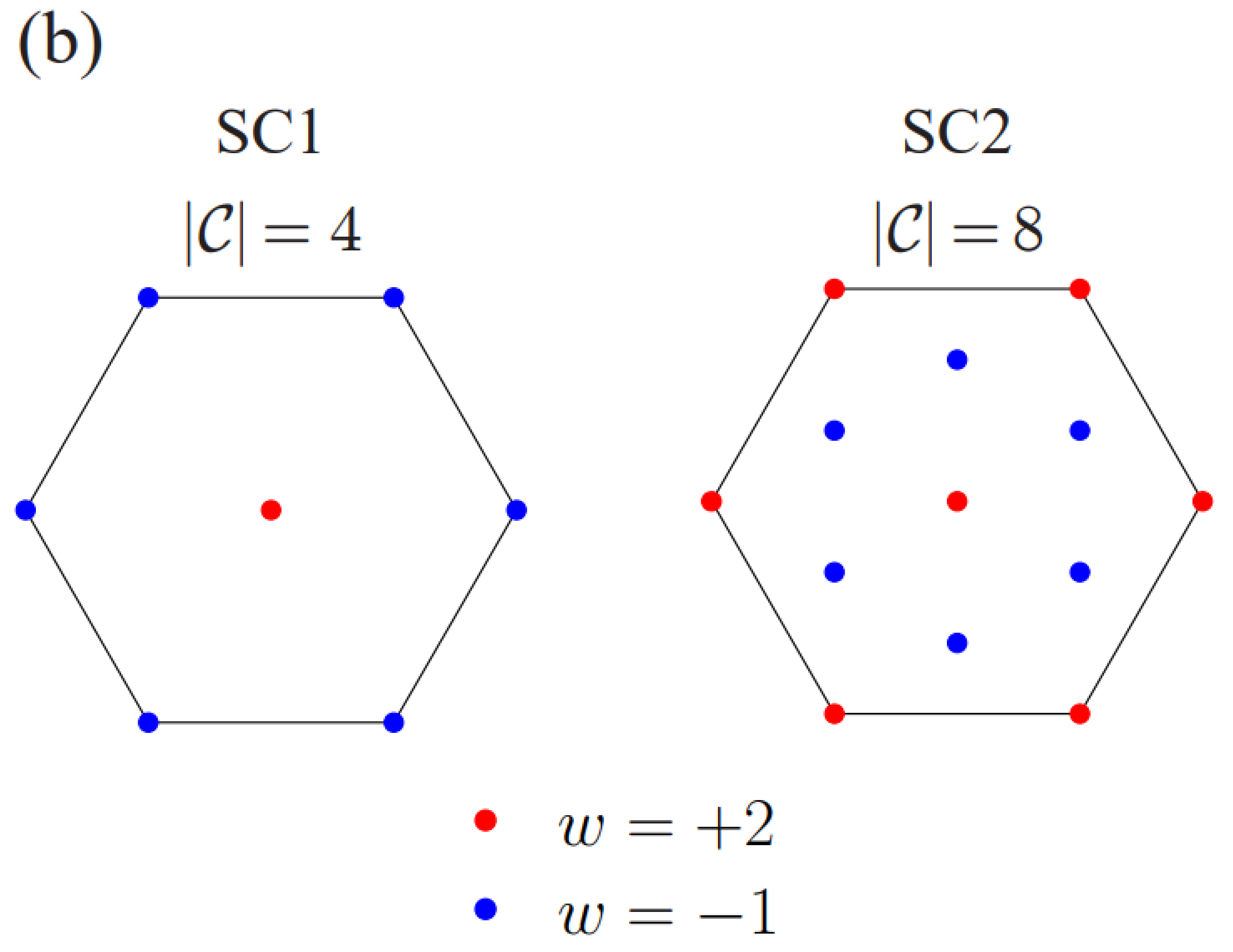

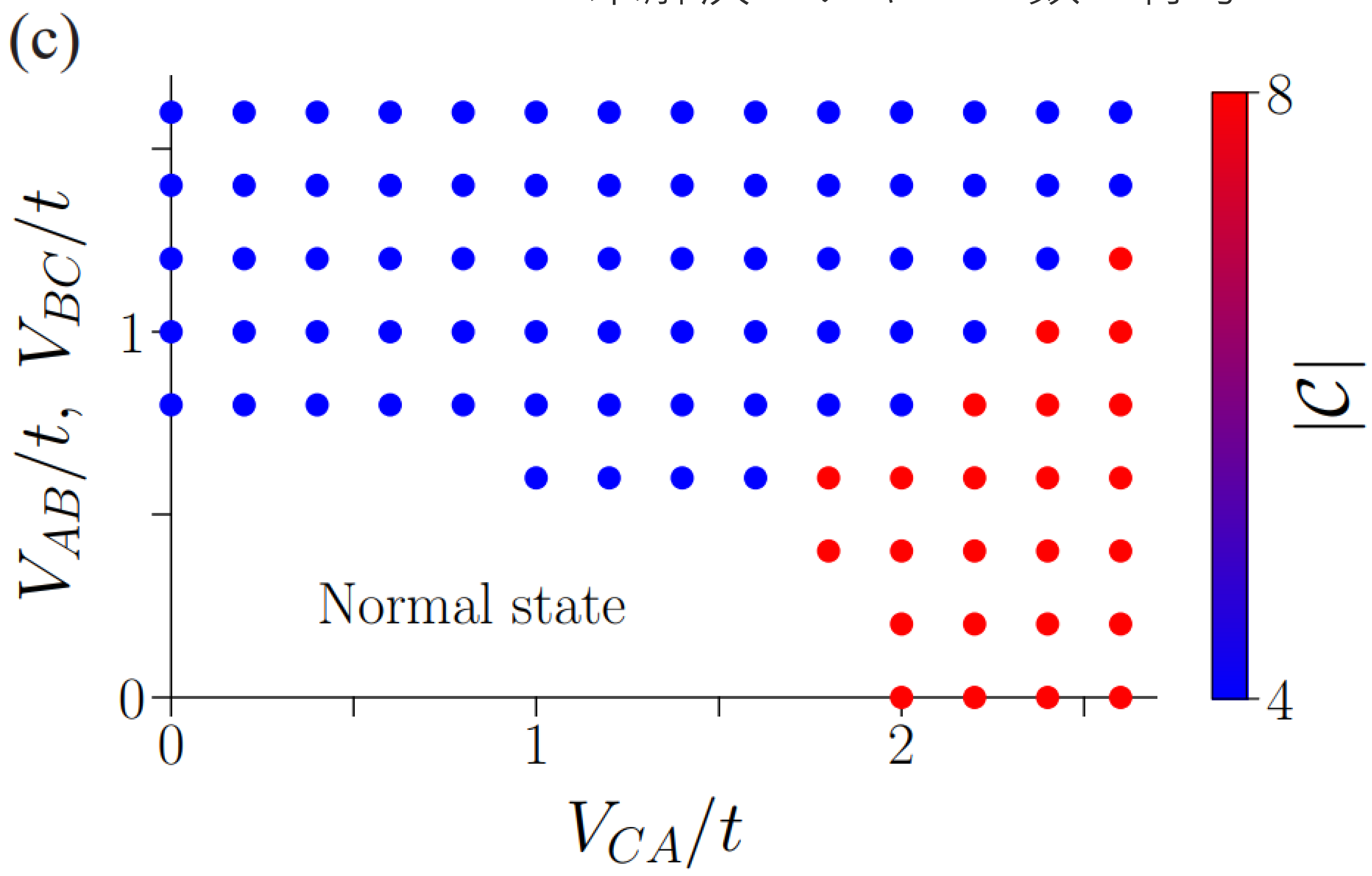

Total Chern number (Fukui-Hatsugai-Suzukiの方法[1]で計算)

$$\mathcal{C} = \frac{1}{2\pi i}\sum_{n=1}^{3}\int_{\mathrm{BZ}} d^2\boldsymbol{k}\left(\frac{\partial A_y^{(n)}}{\partial k_x} - \frac{\partial A_y^{(n)}}{\partial k_y}\right)$$

[1] T. Fukui *et al.*, J. Phys. Soc. Jpn. 74, 1674 (2005)

グラフェンの場合

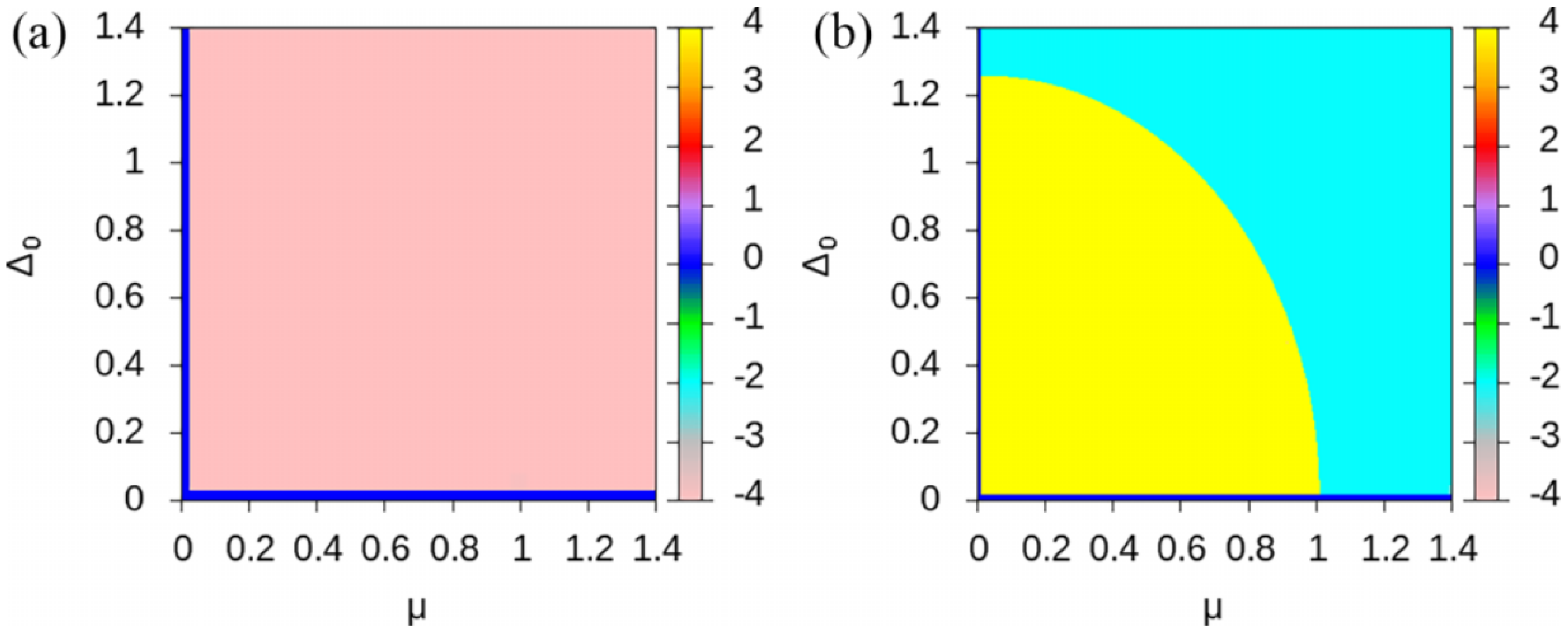

FIG. 3. Chern number $\mathcal{C}$ as a function of μ and Δ_0 for monolayer graphene for the (a) $d + id'$- and (b) $p + ip'$-wave states.

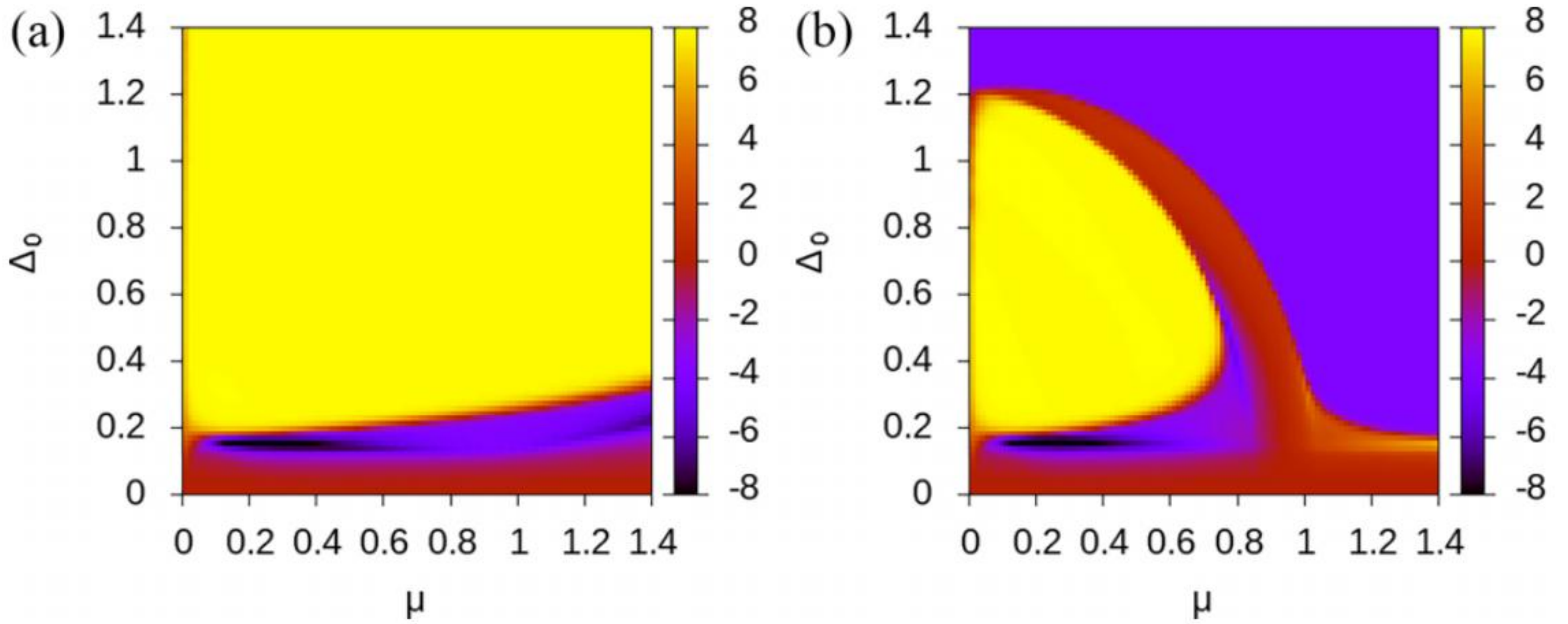

FIG. 9. Chern number $\mathcal{C}$ for AB-bilayer graphene with (a) $d + id'$- and (b) $p + ip'$-wave SC order parameter as a function of μ and Δ_0 at $\gamma_1 = 0.2$ and $\gamma_3 = 0$, with a phase difference $\phi = \pi$ between the SC orders in the two graphene layers.

A. Crépieux *et al.*, Phys. Rev. B **108**, 134515 (2023)

interlayer hopping γ_1

trigonal warping γ_3

気になっていること

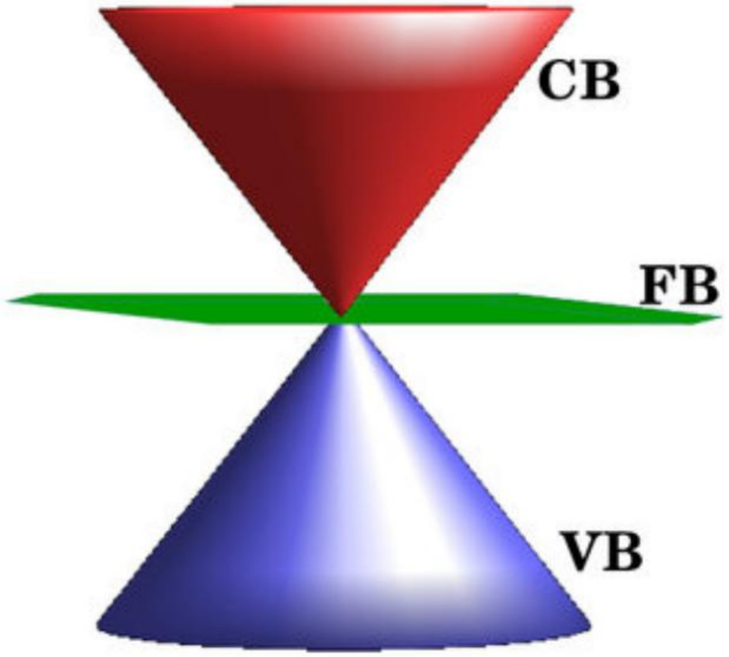

$$H_0(\boldsymbol{k}) = v\hbar k \begin{pmatrix} 0 & e^{i\theta}\cos\varphi & 0 \\ e^{-i\theta}\cos\varphi & 0 & e^{i\theta}\sin\varphi \\ 0 & e^{-i\theta}\sin\varphi & 0 \end{pmatrix}$$

$$\theta = \arg(k_x + ik_y)$$

$$E_\pm(\boldsymbol{k}) = \pm v\hbar k, \quad E_0(\boldsymbol{k}) = 0$$

バルク・エッジ対応（チャーン数に対応したエッジ状態があるはず）
A-C間引力の起源（スピン揺らぎとスペクトル・フラットバンドとの関係）
フラットバンドと量子幾何

Gell-Mann行列で表現されるスピン-1系でディラック・フラットバンドが現れるのはどんなとき？

線形化Eliashberg方程式の固有値 λ

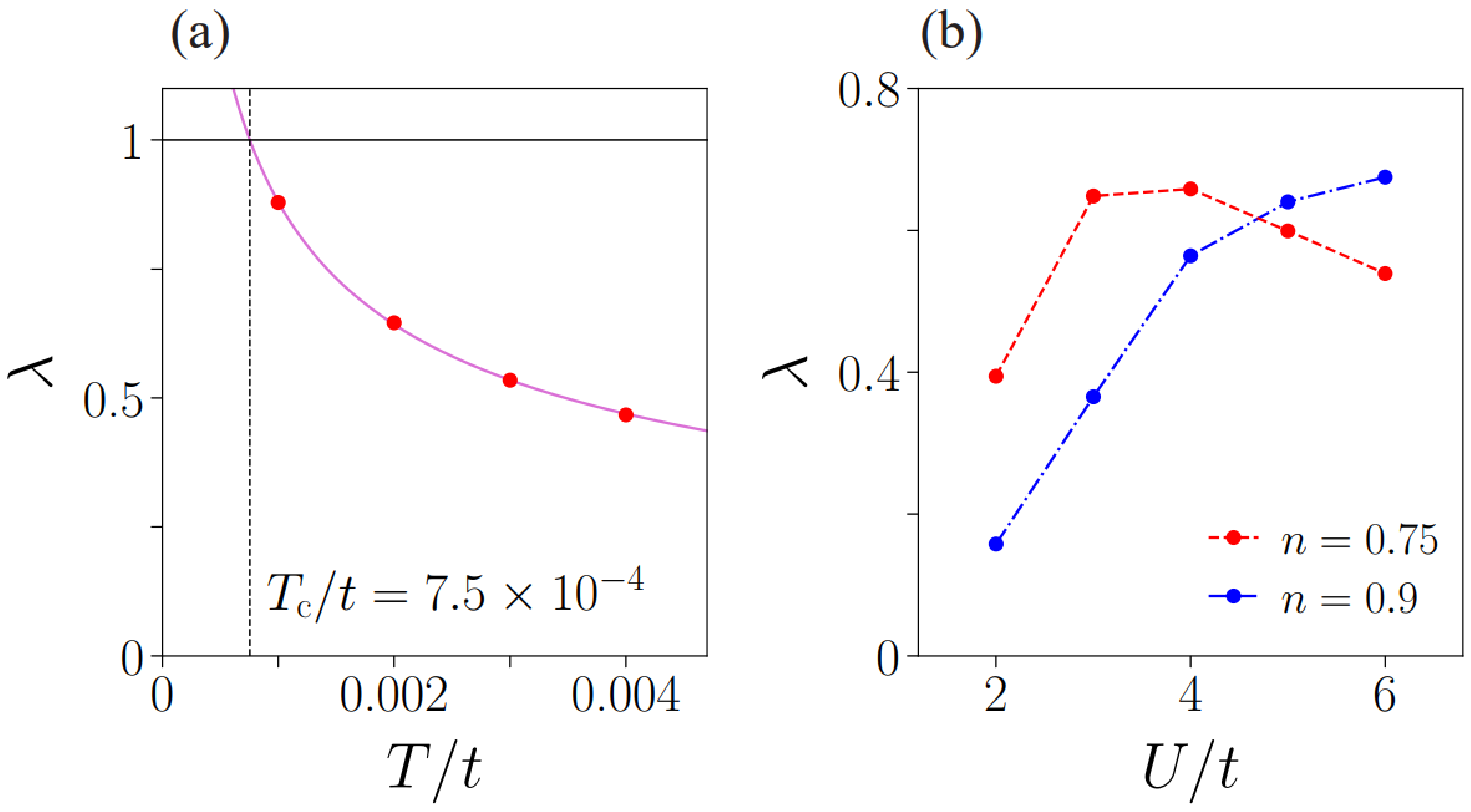

スピントリプレットの固有値